A Review on Explorations of the Oxygen Blast Furnace Process

Zhang, Wei; Dai, Jing; Li, Chengzhi; Yu, Xiaobing; Xue, Zhengliang; Saxen, Henrik

Published in:
Steel Research International

DOI:
10.1002/srin.202000326

Published: 01/01/2021

Document Version
Accepted author manuscript

Document License
Publisher rights policy

A Review on Explorations of the Oxygen Blast Furnace Process

Wei Zhang[1, 2*], Jing Dai[3, 4], Chengzhi Li[1], Xiaobing Yu[4], Zhengliang Xue[3], Henrik Saxén[2*]

1. The State Key Laboratory of Refractories and Metallurgy, Wuhan University of Science and Technology, Wuhan 430081, China
2. Process and Systems Engineering Laboratory, Faculty of Science and Engineering, Åbo Akademi University, 20500 Åbo, Finland
3. Key Laboratory for Ferrous Metallurgy and Resources Utilization of Ministry of Education, Wuhan University of Science and Technology, Wuhan 430081, China
4. School of Metallurgy, Northeastern University, Shenyang 110819, China

*Corresponding authors' E-mail: wei_zhang@wust.edu.cn; henrik.saxen@abo.fi

ABSTRACT

The oxygen blast furnace (OBF) process has been extensively studied theoretically because of the promising energy conservation and CO_2 emission reduction potential. This paper reviews investigations of the OBF process and presents some suggestions for its future development. After a brief historical overview, numerical simulation models of different degree of sophistication (e.g., 0-D, 1-D, 2-D and 3-D models) and regional models are reviewed, stressing the pros and cons of the approaches. Studies focused specifically on minimization of energy, exergy or CO_2 emissions are also treated, as well as on the effect of the feedback loop in furnaces with top gas recycling. Experimental approaches, including laboratory studies of pertinent problems, as well as pilot and industrial trials the OBF process are finally reviewed. The main findings can be condensed into the following: Static and dynamic models of the OBF should be revised to consider the newest theoretical findings in the thermodynamics and kinetics involved as well as the particular limitations of the technology. Models focusing on energy demand and emissions should be further developed and applied to enhance the design for increased efficiency and sustainability of the complicated OBF system. As it will be challenging to operate the full OBF process with top gas recycling (TGR), Mathematical modeling focused on practical operation is therefore warranted and could provide useful tools for tackling control problems and difficulties that will arise in forthcoming industrial trials. A medium oxygen enriched blast furnace with TGR is considered an optimal forerunner since its operation conditions agree more closely with those of the traditional blast furnace. It would furthermore provide a path of transition to the use of the full OBF in industrial scale.

Keywords: Oxygen blast furnace; top gas recycling; mathematical model; industrial trial

1. Introduction

The fast progress of industrial modernization and the development of cutting-edge technologies in various fields have resulted in ever-increasing demands of steel of higher quality. In the traditional ore-based steelmaking process, the blast furnace (BF) is a key processing unit, but its energy consumption is high and a large share of the environmental impact of the steel production chain stems from it and its ancillary units. To keep the BF feasible and competitive in the future, a number of developments have been proposed, mainly including the following three options: 1) Upgrading of the current equipment and adoption of advanced measurement and control technologies for higher operation efficiency. 2) Development of a novel blast furnace smelting process suitable for cleaner separation of paragenetic minerals. 3) New innovative developments of the BF, e.g., the oxygen blast furnace (OBF) process. [1-3] Particularly, the OBF with top gas recycling (TGR-OBF) process attracts more and more interest.

Although most investigators stress the low carbon consumption and high productivity as the main merits of the OBF process, theoretical analysis of these two features have seldom been conducted in detail, especially compared with the traditional BF. It is a well-known fact that the theoretical minimum carbon consumption is the lowest value that still meets the requirements of reducing iron ores and melting metal and slag in a traditional blast furnace (TBF). [4, 5] In this process, a proper direct-reduction degree (30-40%) is necessary to supply the CO as reducing gas in the furnace, although the direct-reduction reaction is endothermic and causes an increase in the coke rate. By contrast, in the TGR-OBF, a lower direct-reduction degree and a lower carbon consumption is achieved because the partial pressure of CO is higher in the furnace, which increases the indirect reduction rate considerably. Simultaneously, the endothermic direct-reduction reaction is unnecessary because the recycled top gas supplies heat and reducing gas, so the direct-reduction is suppressed, which lowers the energy demand.

Because of the absence of nitrogen, the bosh gas volume in the OBF decreases dramatically. Even for the case with top gas recycling, it is still much lower than the bosh gas volume of the TBF. From a fluidization/flooding point of view, this decrease in volume is favorable as it facilitates a higher production rate.

In summary, the OBF process is an emerging ironmaking process pursuing very low carbon dioxide emissions and low energy consumption. It is characterized by the following benefits:[6-13]

(1) The environmental impact is drastically decreased. Little nitrogen oxide (NO_x) is generated and discharged in the hot stove because a nitrogen-free blast is applied. In parallel, the decrease in coke requirements will reduce the pollution caused by the coking process.

(2) Productivity and pulverized coal injection rate are improved. With various technical measures, the productivity of OBF can be increased substantially (by 30-200% according to different estimates). In addition, the pulverized coal rate can be increased because of the higher oxygen content in the combustion zone, which will lower the dependence of metallurgical coke.

(3) Indirect reduction degree is improved and fuel rate decreases. The reduction condition in the blast furnace is similar to that in the shaft furnace: an increase in the indirect-reduction degree yields a corresponding decrease in the direct-reduction degree and a dramatic decrease in fuel rate.

(4) The quality of top gas is improved and the CO_2 in it is captured. The calorific value of top

gas from an OBF almost doubles compared with that of a traditional blast furnace, and the CO_2 capture substantially lowers the emissions of the process.

This paper provides a review and critique of fundamental research work on the OBF, including mathematical modelling and experimental studies. The models are divided in different categories based on the spatial distribution considered, treating models with particular focus on minimization of the energy or exergy demand, or CO_2 emissions, separately. The effect of the feedback loop in furnaces with top gas recycling, and the feasible operation window are also treated. This provides an overview of numerical means of analyzing the new process. The experimental work is divided into laboratory studies and pilot or (semi-)industrial trials, where the former are focused on sub-problems or phenomena of particular interest in the OBF. Based on the review, some suggestions are presented for future development work of the OBF process.

2. History of Development of the OBF Concept

In general, the OBF process refers to an ironmaking process with the injection of highly oxygen enriched or even full oxygen blast instead of slightly oxygen-enriched preheated blast used in the traditional blast furnace. In the narrow sense, OBF only refers to the full oxygen blast furnace (FOBF) but in a broader sense also to what could be referred to as medium oxygen enriched blast furnace (MOBF) or other highly oxygen-enriched blast furnaces. The OBF process is usually combined with top gas recycling:[14-17] the three main categories, TBF, TGR-MOBF and TGR-FOBF are depicted schematically in Figure 1. In studies of the concepts, carbon dioxide is sometimes stripped off the recycled top gas and sometimes not. In cases where the top gas is not recycled, natural gas, coke oven gas (COG) or other hydrogen-enriched reducing gas is sometimes injected instead.

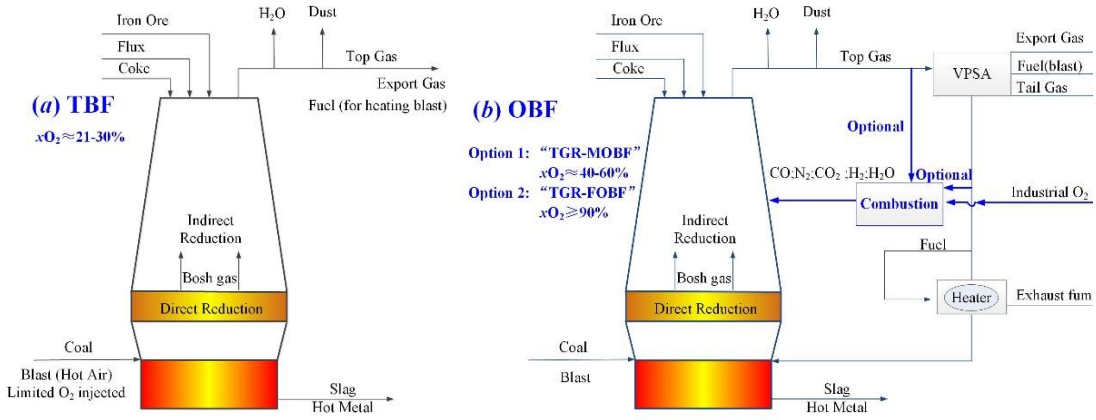

Figure 1 Schematic diagram for TBF and OBF

It is interesting to note that the prelude to the OBF process was a BF with injected hot reducing gas without substantial oxygen enrichment. According to the review by van der Stel et al.,[16] Lance first developed this concept in the 1920s, and found that the reducing gas volume in the raceway could be compensated by injecting preheated reducing gas (27% CO, 33% H_2, and 26% N_2) at 1000˚C. As a result, the coke rate could be decreased by 70%, at that time corresponding to 345 kg per ton hot metal (thm). In the early 1970s, this concept was tested in pilot experiments with a 4.6

m hearth diameter BF,[16] where reformed reducing gas at 1000°C was injected into the lower shaft. The author reported a replacement ratio of 0.22-0.26 kg coke/Nm^3.

In 1972, Wenzel et al.[18] applied for an American patent about the OBF process proposing an ironmaking process with nitrogen-free blast. In this process, high concentrated nitrogen-free reducing gas was generated from upgraded top gas, and was then divided into two flows when it returned to the furnace. One was recycled to bosh tuyeres, and the other was injected into tuyeres in the lower stack.

Also in the OBF process proposed by Fink,[19] two rows of tuyeres were arranged on the hearth and lower shaft of the blast furnace. Oxygen and auxiliary reductants were injected into the furnace synchronously, and part of top gas deprived of CO_2 and dust was recycled and also blasted into the tuyeres. The remaining top gas was provided for other uses in the plant. Based on Fink's calculations, this process was theoretically predicted to achieve a coke rate below 150 kg/thm at a pulverized coal rate of more than 400 kg/thm.[20]

Lu[21] proposed an OBF process of high productivity, estimated to be 30-100% higher than in the TBF. However, this process also had some disadvantages, including its relatively high fuel rate and large oxygen consumption. Furthermore, the Lu OBF process was operated under the hypothesis that the direct-reduction degree was zero. According to Lu, the coke rate, coal rate, and the bosh gas volume and oxygen demand were 250 kg/thm, 450 kg/thm, 1064 Nm^3/thm and 355 Nm^3/thm, respectively, and the theoretical flame temperature was 2360°C when 10% of the top gas was recycled.[22]

In the FOBF process proposed by Qin et al.[23] a part of the top gas was deprived of CO_2 by carbon propyl ester, and then heated to 1200 K for recycling through upper tuyeres (located at the lower shaft). The remaining top gas without CO_2 deprivation and heating was used as the carrier gas for pulverized coal injection in the hearth tuyeres to adjust the flame temperature.

By contrast, in the Poos process,[24] which was operated without top gas recycling, a large volume of gas was generated in the raceway by injecting excessive pulverized coal to reach a balance of the shaft heat demand. Steam injection was applied to maintain a reasonable theoretical flame temperature. Likewise, the balanced oxygen blast furnace (BOBF) process proposed by Ma and Edström[10,25,26] was also operated without top gas recycling. The oxygen content of the blast varied from 40% to 90% without blast preheating in hot stoves, but with massive pulverized coal injection, and the consequent top gas temperature was calculated to be sufficiently high (120°C).

Gao et al.[27] put forward a process named Oxygen-Coal-Flux (OCF) process, which was operated without hot stoves as well. The top gas without CO_2 deprivation and heating, but cleaned, was recycled as a carrier gas for massive coal and moderate flux injection. In the less-gas-circulation (LGC) OBF process proposed by Zhang,[12] a portion of the top gas without CO_2 deprivation was heated after dust removal, and then recycled through tuyere injection. The remainder of the top gas served as fuel to heat the recycled gas.

As a summary, a brief comparison between the OBF processes mentioned above is provided in Table 1. Generally, all the OBF processes listed in the table can, to some extent, improve productivity, increase the indirect-reduction degree and decrease the fuel rate and coke rate, thus achieving the goal of reducing CO_2 emissions. To be specific, in terms of the techniques of solving the uneven heat distribution in the OBF (*i.e.*, thermal shortage in the upper region and excess heat in the lower), these OBF processes are categorized into different groups. For example, to solve the thermal shortage in the upper region, Fink and FOBF processes directly supply heat to the upper

region of the OBF through injecting oxygen and pulverized coal synchronously, or hot recycled top gas, into the shaft or bosh. In the Lu and Poos OBF processes, the excessive heat in the lower region is transferred to the upper region through increasing the amount of gas generated in the lower regions. In the OCF process, the heat consumption in the shaft region is decreased through changing the flux feeding position from the furnace top to the hearth. To solve the overheating of the lower region of the OBF, the Fink and Lu processes use a large amount of CO_2-deprived top gas injected into the hearth to physically absorb the excessive heat and then transfer this to the shaft, where it is required. The FOBF, Poos and OCF processes, in turn, use steam or top gas without CO_2 deprivation injected into hearth to chemically absorb the massive heat in the lower region by strong endothermic reactions (the Boudouard reaction $C+CO_2 \rightarrow 2CO$, and the water-coke reaction $H_2O+C \rightarrow CO+H_2O$). Consequently, due to different techniques used in these processes, it is expected that the key process performance and economic indices, such as indirect-reduction degree, coke rate and fuel rate, should be different.

Strictly speaking, in the history of OBF process development, no fundamentally new concepts have been proposed after the 1990s, even though smaller steps of development indeed have been taken. The possible options offered by different variants of the OBF processes make the choice of concept for future development challenging. However, the characteristics of each of the above processes should be carefully considered in order to guarantee that a suitable (or in the best case, optimal) process is selected for the specific industrial practice in question.

Table 1. Comparison of different early OBF processes.

Year	Name of OBF process	Gas injection position	Gas composition	Technique characteristics
1972	Wenzel [18]	Hearth and lower shaft	Oxygen + fossil fuel + recycle upgraded top gas at two rows of tuyeres	Fossil fuel reacted with top gas and the upgraded gas was injected by two options: into the hearth tuyeres, or into both lower shaft and hearth tuyeres.
1978	Fink [19]	Hearth and lower shaft	Oxygen + pulverized coal + recycle top gas at two rows of tuyeres	Recycle top gas is deprived of CO_2. No heating of the recycle top gas. Low fuel rate and oxygen consumption rate. Productivity is improved by 50% but the injection rate is low.
1984	Lu [21]	Hearth	Oxygen + pulverized coal + recycle top gas	Recycle top gas is deprived of CO_2. No heating of the recycle top gas. High coal injection rate and a large amount of supplied gas.
1985	FOBF [23]	Hearth and lower shaft	Recycle top gas at lower shaft; Oxygen + pulverized coal + recycle top gas at hearth	Top gas, deprived of CO_2 by carbon propyl ester, is heated to 1200 K and recycled through the upper tuyeres. Top gas without CO_2 deprivation and heating is used as a carrier gas for coal injection into hearth.
1990	Poos [24]	Hearth	Oxygen + pulverized coal + vapor	No top gas recycling. Excessive coal injection to balance the shaft heat demand. Steam injection to maintain a reasonable flame temperature.
1992	BOBF[25,26]	Hearth	Oxygen + pulverized coal + nitrogen (or air + oxygen)	No top gas recycling. Oxygen content of the blast varies from 40% to 90%. Excessive coal injection, without hot stoves.
1994	OCF[27]	Hearth	Recycle top gas + oxygen + pulverized coal + flux	Top gas without CO_2 deprivation and heating. Top gas is recycled as carrier for coal and flux injection after purification. No hot stoves needed.

Today, the TGR-OBF process is widely regarded as a potential future energy- and emission-saving variant of the BF process since the role of coke and pulverized coal as reducers and thermal suppliers is partially substituted by recycled top gas to the hearth and shaft. A computational example of the flows in the full oxygen blast furnace with top gas recycling is presented in Figure 2 based on the calculation of Zhang et al.[28] The process is operated with a blast oxygen content of

98%, coke rate of 200 kg/thm, blast temperature of 500°C, shaft and hearth gas recycling ratios of 30% and 60%, respectively, and shaft gas and hearth gas injection temperatures of 900°C and 1200°C, respectively. The calculated coal rate is 205 kg/thm under the mass and heat balance constraints applied. The flows of ore, dust, top gas, recycling gases etc. are also calculated.

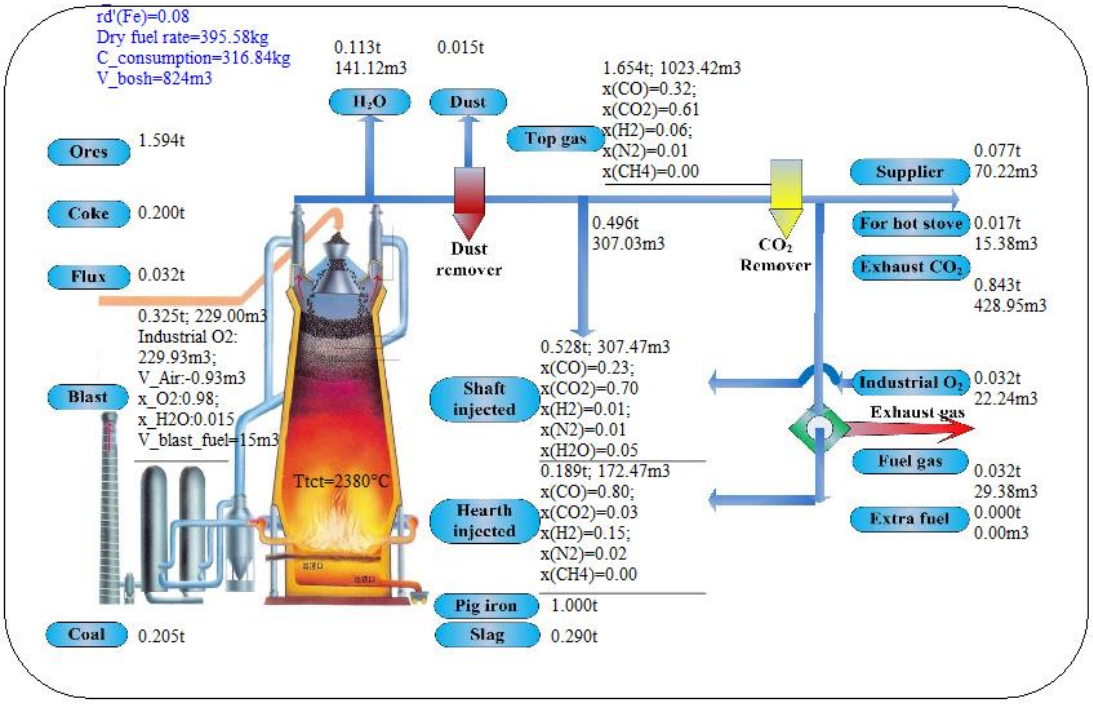

Figure 2 Flows of the TGR-FOBF process [28]

The thermal balance of the TGR-FOBF process with the same operation condition was calculated as shown in Table 2. The energy of both shaft and hearth recycled gas accounts for 24.6% in the total thermal balance. The fuel rate of the TGR-OBF process in this case decreases by 93 kg/thm compared to the TBF process. The role of coke and pulverized coal as reducer and thermal supplier is substituted by shaft and hearth recycled gas, and result in the final fuel savings.

Table 2 Thermal balance for the steady TGR-FOBF process [29]

Items	GJ/thm	%
Heat input:		
1. Calorific value of coke	6.042	36.92
2. Calorific value of coal	6.145	37.55
3. Heat of the hot blast	0.152	0.93
4. Energy of the shaft recycled gas*	1.611	9.84
5. Energy of the of hearth recycled gas*	2.413	14.75
Total heat input	16.364	100
Heat output:		
1. Heat of oxides decomposition	6.785	41.46
2. Heat consumed in S deprivation	0.008	0.05
3. Heat of carbonates decomposition	0.052	0.32
4. Heat of coal decomposition	0.183	1.12
5. Enthalpy of slag	0.55	3.36
6. Enthalpy of hot metal	1.3	7.94
7. Enthalpy of top gas	0.296	1.81
8. Calorific value of top gas	5.025	30.71
9. Calorific value of un-combusted C	1.436	8.78
10. Heat consumed in H_2O evaporation	0.324	1.98
11. Heat loss	0.404	2.47
Total heat output	16.364	100

*Note: Energy of the shaft recycled gas includes both calorific value and enthalpy of the shaft recycled gas, and similarly for the energy of the hearth recycled gas.

3. Numerical Simulation of OBF

In this chapter, we classify OBF simulations into three categories according to different objectives, focused upon 1) physicochemical mechanisms during the reduction and melting process in the furnace, 2) minimization of energy and exergy demand, and greenhouse gas emissions, as well as 3) OBF dynamics and feasible operation points. It should be noted that the categories are overlapping, since the analyses in the second and third items are based on models treated under the first item.

3.1. *Detailed Process Models of OBF*

3.1.1 Zero-dimensional Models

Overall or two-zone models of OBF are usually regarded as zero-dimensional (0-D) models. Such models of the OBF form the foundation not only for designing operation parameters of the process but also for acting as references for multi-dimensional dynamic models. Thus far, a series of studies[30-37] on steady-state operation of the OBF process have been conducted with such models, mainly based on mass and heat balance equations. However, some crucial issues still remain to be explored. These are partly due to the simplified form of the models which requires fundamental assumptions concerning boundary conditions used in the calculations.

(1) Direct-reduction Degree

The direct-reduction degree was assumed as zero for the calculation in the Lu OBF process.[21] When the OBF process is narrowly regarded as a full oxygen blast furnace with a

similar reduction intensity to that of shaft furnaces, this hypothesis is reasonable. Nevertheless, when it comes to the general concept of the OBF process with highly oxygen-enriched blast, this assumption is obviously not appropriate and should be avoided.

(2) Thermal Reserve Zone Temperature

The gas injected from raceway rises inside the blast furnace and exchanges heat with the descending solid and liquid phases. Initially, the gas temperature is higher than that of the burden. When the gas ascends through the direct-reduction region, the strongly endothermic Boudouard reaction (solution loss reaction) occurs and the gas temperature decreases dramatically. Also, the melting of the ores act as a heat sink. Consequently, a thermal reserve-zone region appears, typically at a temperature ranging from 900˚C to 1000˚C. Na[38] selected 950˚C as the boundary temperature in the study of a zonal thermal balance of the traditional blast furnace. Recently, zonal static models have been applied extensively in studies of the OBF, using different boundary temperatures (927˚C, 950˚C, 1000˚C, etc.).

It may be argued that the temperature range for the thermal reserve zone in the OBF is important and that it reflects the operation of the process, so the value cannot be freely chosen. First, with hot gas injected into shaft or hearth, the strong heat exchange between gas and burden will be delayed (from the view of the ascending process of the gas) because the high indirect reduction degree achieved in the lumpy zone constrains the direct-reduction degree of the ores in high-temperature region. Consequently, the thermal reserve zone is shifted upwards and the temperature of this region increases. This can be seen from the results of Ohno's one-dimensional dynamic OBF model.[6] Second, without heat-carrying gas injected into the shaft or hearth, the direct-reduction degree will rise because the temperature of the upper shaft cannot meet the thermodynamic requirement of the indirect-reduction reaction, compared with the traditional blast furnace. Thus the Boudouard reaction in the high–temperature region initiates a strong heat exchange between gas and burden. This deduction is consistent with the results of Yamaoka's one-dimensional OBF model.[8]

Considering the above, the change in the temperature of thermal reserve zone indicates that most of the predictions by the current static OBF models may be inaccurate. Figure 3 shows the heat balances of the overall and zonal OBF with a thermal-reserve-zone temperature of 950˚C.[22] It can be seen that the overall heat balance can be satisfied while the zonal one cannot when top gas is not recycled. A similar result at a thermal-reserve-zone temperature of 1000˚C was also presented by Guo et al.[33] However, if the boundary temperature is decreased, the zonal heat balance may be satisfied due to the decreased heat input into the high-temperature zone and increased heat input into the lumpy zone. In these two-zone models, the total heat input/output of whole BF was usually not equivalent to the sum of heat input/output of the partial parts, which causes confusion (Figure 3). We attribute this to the different calculation rules between the total heat balance and the regional heat balance. For instance, the chemical energy was calculated in the high temperature zone but was not taken into account in the total heat balance.

The study of Yamaoka[8] suggested that although the OBF process without top gas recycling requires more energy, it may still be feasible and that the feasibility of FOBF process is more dependent than the TBF on local heat balance constraints.

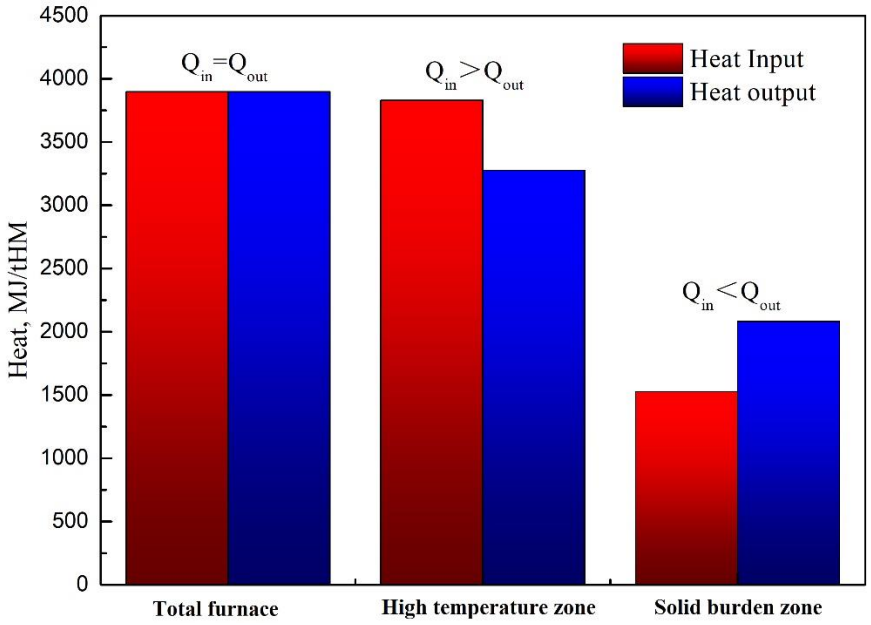

Figure 3. Overall and zonal heat balances of an OBF with a thermal-reserve-zone temperature of 950°C.[22]

(3) Productivity of OBF

Based on the simulation results of one-dimensional models and the data from industrial trials, the productivity, namely the utilization coefficient of the OBF process, turns out to be 30-200% higher than that of that of TBF.[6] However, such a high productivity may not have been taken into account appropriately in the balance calculations of the early models.

(4) Heat Loss of OBF

Compared with the TBF, the heat loss per ton hot metal decreases in the OBF due to the increased productivity, and this has also been demonstrated by the industrial trials of NKK. It is not clear whether this decrease in the specific heat loss has been taken into account in earlier balance calculations of the OBF.

(5) Upper Limit of Pulverized Coal Rate of OBF

Pulverized coal injection is an important means to decrease the coke consumption and also to adjust the combustion temperature of the raceway: by increasing the injection rate, the flame temperature decreases.

The ratio of coal to oxygen (coal/O_2) corresponding to the incomplete combustion to CO in the raceway equals about 1.5 kg/Nm^3, indicating that the coal injection rate is not unlimited. According to the studies of Miyazaki et al.,[39] when the oxygen content of the blast was 75%, the upper limit of the coal/O_2 ratio that could guarantee a favorable combustion of coal was 1.2 kg/Nm^3. As the ratio further increased, the combustion rate increased slowly or even leveled off. Compared with the critical ratio, O_2 was considered excessive when the ratio was ≤ 1.2 kg/Nm^3. The corresponding coal injection rate and oxygen consumption were 360 kg/thm and 300 Nm^3, respectively. Zhang[12] also reported that the combustion rate of coal increased with increasing oxygen-to-carbon ratio (ξ). The combustion rate of coal depended linearly on the partial pressure of oxygen for ξ = 1.5-2.0, but the combustion rate grew less as ξ further increased.

3.1.2. *One-dimensional Models*

The spatial distribution of state variables of OBF process are not considered in the over-all or two-zone models. In order to illustrate and gain deeper understanding of the inner process of the OBF, one-dimensional (1-D) models have been established.

In 1990, Matsuura et al.[6,7,40] established a one-dimensional model of an OBF with preheated gas injection into the shaft. According to the results of the model, the temperature of thermal reserve (T_R) depended on the flow rate (V_b) and temperature of the preheated gas (T_b), by contrast to the conditions in the TBF. Figure 4 illustrates the variation in the temperature of the thermal reserve zone and the direct-reduction degree with increasing temperature of the injected gas.

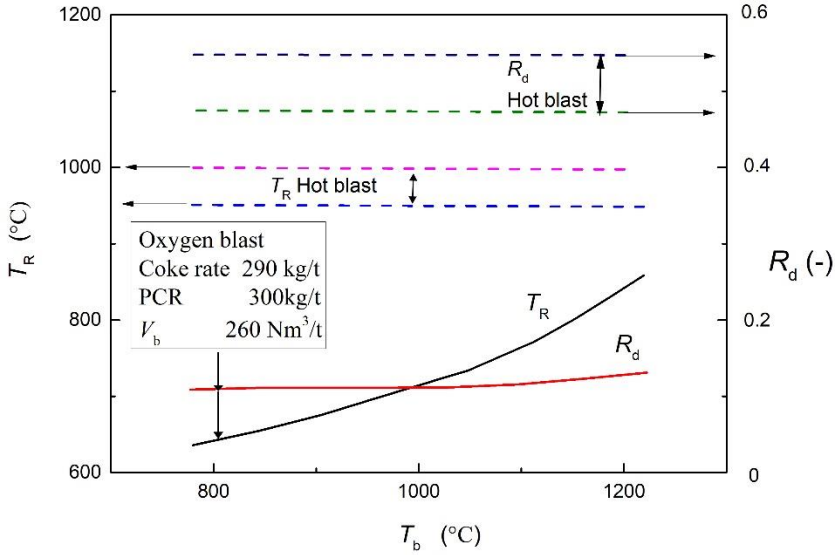

Figure 4. Effect of gas preheating temperature (T_b) on the solid temperature of thermal reserve zone (T_R) and direct-reduction degree (R_d).[7]

The data was obtained under a specific oxygen flow rate of 260 Nm^3/thm, coke rate of 290 kg/thm and pulverized coal rate (PCR) of 300 kg/thm in the OBF process. It can be seen that the temperature of thermal reserve zone rose significantly, while the direct-reduction degree rose only slightly with increasing temperature of the preheated gas, T_b. As T_b increased from 800°C to 1200°C, the temperature of the thermal reserve zone increased from 630°C to 850°C, which agrees with the inference results mentioned above.

In 1990 and 2001, a one-dimensional shaft model[41] was applied to the solid-phase regions of FOBF and LGC-OBF by Qin et al.[42] and Zhang,[12] respectively, combined with a description of the thermochemistry, yielding quite comprehensive models of the OBF process.

In 1992, Yamaoka and Kamei[8] established a one-dimensional model of OBF without top gas recycling by dividing the blast furnace into three regions, including the hearth, the raceway and the effective reaction regions, taking heat exchange between gas and burden into consideration. It was assumed that only hot oxygen-enriched blast was blown into the raceway. The blast temperatures were set at 30°C, 600°C and 1200°C, respectively, and the corresponding theoretical minimum fuel rates were determined. As the oxygen content increased, the indirect-reduction degree rose first but then dropped, while the fuel rate dropped first before it rose.

In 1995, Tang and Xu[43] presented a one-dimensional model of the OBF process with preheated gas injection in the shaft based on the rate equations proposed by Yagi,[44] Hatano et al.[45]

and Bi.[46] The modelling results showed that with the increases in the volume flow rate and temperature of the preheated gas, the temperature of the burden in the upper shaft increased. In contrast, the composition of the preheated gas did not have a significant effect on the heat distribution in the lumpy zone.

More recently, in 2016, Jin et al.[47] presented a one-dimensional comprehensive model, comprised of the stack and bosh, combustion zone and gas recycling system for prediction of the thermo-chemical processes, energy consumption and carbon emission of the TGR-OBF. The modelling results indicated that compared with the TBF, the CO concentration was increased and the overall temperature was lowered in a TGR-OBF, which is advantageous for reducing the reaction of coke and increasing the reduction rate of iron oxides. The energy input to the TGR-OBF could be reduced by 5-30% compared with the TBF, due to the effective utilization of the recycled gas. Furthermore, the TGR-OBF process could provide sufficient carbon reductants into the furnace, although its total carbon input was lower than for the TBF. The CO_2 emission in the TGR-OBF process was also significantly reduced. Compared with the TBF, the net CO_2 emission in the TGR-OBF process could be decreased by about 35%.

3.1.3. *Two-dimensional Models*

Taking the burden and gas flow, heat and mass transfer and chemical reactions into account, Ohno et al.[6] established a two-dimensional (2-D) mathematical model for the OBF process, which was similar to the model proposed by Kuwabara et al. in the 1980s.[48] In this model, the calculation was based on NKK's Fukuyama No.4 blast furnace (4,288 m^3). According to the simulated data of burden temperature and reduction-degree distribution, it was concluded that as the temperature of the preheated gas (300 Nm^3/thm) increased from 800°C to 1200°C, the temperature of burden increased and thus the burden could be heated to a larger extent. Furthermore, the overall reduction degree on the burden also increased. Thus, elevating the temperature of the injected gas was beneficial for the process.

Based on the simulation results, it was also shown that with a lowered gas injection position, the inner temperature of the blast furnace decreased. Consequently, the reduction reaction was incomplete due to insufficient heat in the furnace stack. The reason for the decreased injection temperature was that the gas injected into the shaft was oxidizing. If the injection position of the oxidizing gas was lower than the thermal reserve zone, the reduction process in the shaft would deteriorate. This explanation matches the results of previous studies.[49,50]

In 2015, Zhang and his partners [51-53] established a 2-D mathematical model based on CFD technology to study the reduction process of the OBF. The estimated reduction state of the solid materials is presented in Figure 5. The authors studied the effect of shaft tuyere position, recycling gas temperature and recycling gas allocation on the reduction behavior of the iron ores. The results indicated that the lower the furnace shaft tuyere position is, or the higher the recycling gas temperature or recycling gas allocation ratio is, the higher the reduction degree at a given position in the furnace.

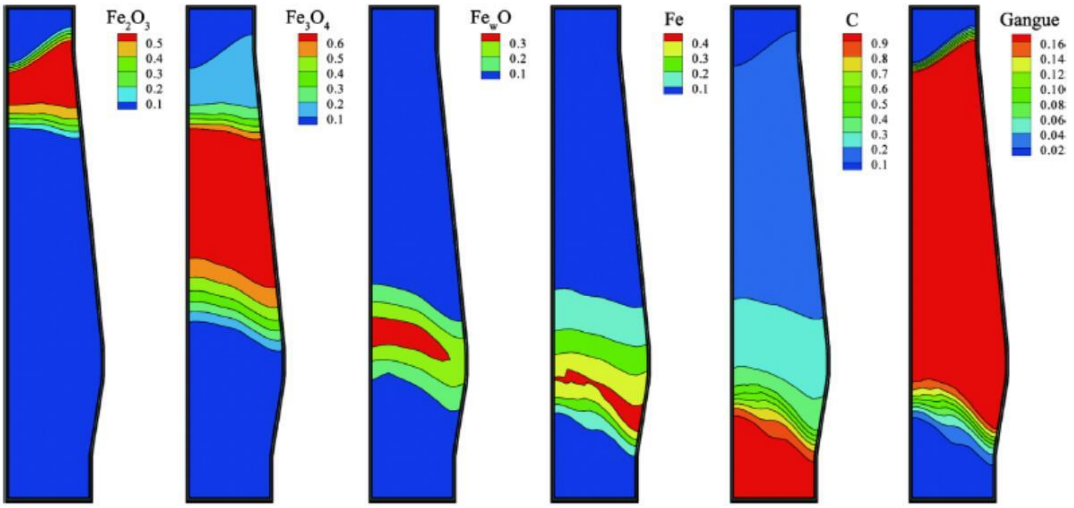

Figure 5. Simulated mass fraction distributions of solid components in the OBF [51]

In 2018, Liu et al.[54] investigated the effect of the flowrate of recycled gas (FRG) on the in-furnace status, productivity and energy consumption. A 2-D axisymmetric CFD model was developed to simulate the gas flow, heat and mass transfer between the gas and solid phases and chemical reactions under varying FRG conditions. In the simulations, the top gas stripped of CO_2 and heated to 900°C was recycled and injected at the hearth tuyeres and in the lower shaft. A three-interface unreacted shrinking core model was used to describe the gas-solid reactions. It was found that the overall temperature, CO concentration, and degree of reduction in the OBF rose significantly with increasing FRG (from 300 Nm^3/thm to 600 Nm^3/thm) in the shaft. The productivity of OBF increased by 5-35%, compared with that of TBF, under varying FRG conditions and the energy savings reached 27-36% when different criteria for energy consumption were considered.

In 2018, Li et al.[55,56] applied a steady-state, axisymmetric multi-fluid model to study a novel OBF process facilitated with belly injection of reformed COG or hot charge of the burden. The research findings indicated that both belly injection of COG and hot burden charge decreased the consumption of carbonaceous materials and increased productivity. The belly injection of COG could improve the indirect reduction by H_2, but the influence was limited to a region near the wall due to the shallow penetration depth. This is probably because the ratio of the belly injected COG flowrate to the total gas flow was relatively small (X = 8 Nm^3/min /(32.8 Nm^3/min) ≈ 0.24). Based on the conclusions by Dong et al.,[57] the belly-injected gas could not penetrate into the central shaft region for a large distance with such a low ratio. In contrast, hot charge of burden could significantly improve the thermal state throughout the entire dry zone of the OBF. Therefore, it can be expected that burden hot charge is a good option if the value of X must be limited to a low range in the OBF process. However, handling of hot burden is a challenge in the practical operation.

More recently, in 2020, Yu and Shen[58] established a 2-D mathematical model to investigate the influence of oxygen enrichment in the range of 1.5-12% on the smelting behavior of an OBF without top gas recycling. It was concluded that the blast rate decreased by 85 m^3/min and oxygen rate increased 92 m^3/min with for every 1 % increase in the oxygen enrichment. At the same time, the CO concentration increased by 1.04% and the flame temperature increased by 58 K. Figure 6 shows the evolution of gas temperature distribution in the blast furnace with increasing oxygen

enrichment. It can be seen the temperature of lumpy zone decreases and the temperature of high-temperature zone increases with the oxygen enrichment. This phenomenon is consistent with the results provided by the 0-D and 1-D models.

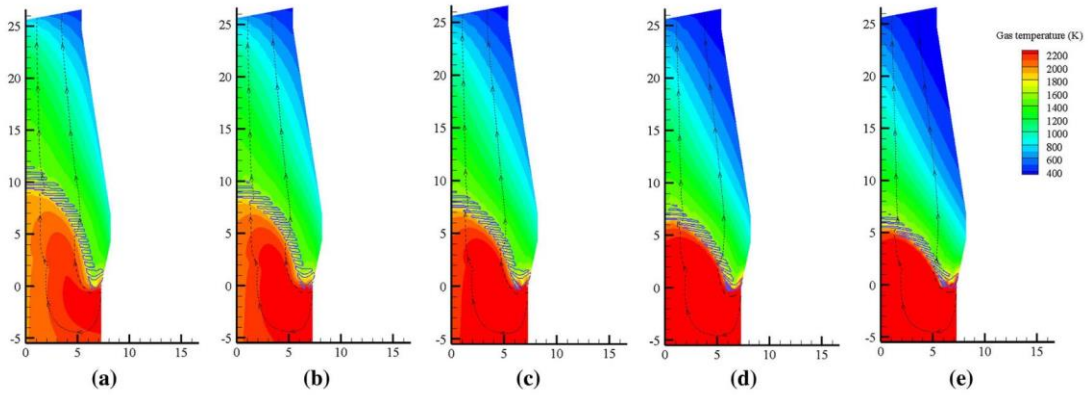

Figure 6 Evolution of thermal condition with oxygen enrichment of (a) 1.5% (b) 3.5% (c) 5.5% (d) 7.5% (e) 9.5%[58]

3.1.4. *Three-dimensional Models*

Three-dimensional (3-D) mathematical models of the TBF were first established in Japan in the 1990s. Since then, 3-D numerical studies of the blast furnace have been conducted by an increasing number of ironmaking researchers.[59-63] In general, based on the multi-phase theory, the matter in the blast furnace could be divided into five phases, i.e., gas, solids, powder, hot metal and slag. Momentum, heat and mass balance equations for the different phases were stated and solved using the finite element method. [64]

In 2013, Chu and his collaborators [65-67] conducted a 3-D simulation study of the OBF process with COG injected through hearth tuyeres. Figures 7 and 8 respectively illustrate the temperature distributions of solid burden and reduction degree under different oxygen contents conditions. Since the ratio of ore to coke under these conditions varied from 4.48 to 6.17, the oxygen content and the flowrate of COG accordingly changed from 24% to 99.52% and from 0 kg/thm to 125.4 kg/thm, respectively, in order to keep the theoretical combustion temperature constant (at 2179°C). As shown in Figure 7, as the oxygen content increased, the high-temperature region of the burden was shifted downwards and the indirect-reduction degree in the shaft increased. As the oxygen content increased, the reduction potential of the injected gas rose, yielding an improved reduction capacity of it as illustrated in Figure 8. As for other effects, as a consequence of the increasing ore-to-coke ratio, the volumetric production rate rose from 2.07 t/(d·m^3) to 3.08 t/(d·m^3) and hence the productivity significantly improved. This shortens the average residence time of the burden, which, in turn, decreases the indirect-reduction degree. However, these two opposing effects practically offset each other, resulting in little change in the indirect-reduction degree.

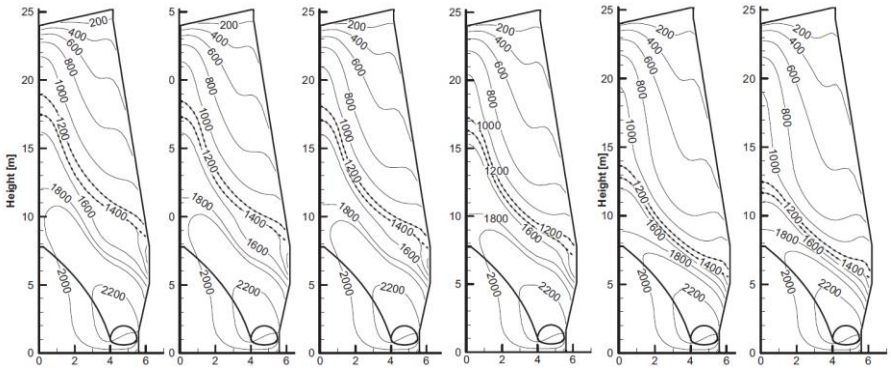

Figure 7. Distribution of in-furnace solid temperature (°C). Oxygen content: (a) 24%; (b) 29.02%; (c) 35.16%; (d) 46.14%; (e) 65.01%; (f) 99.52%.[65]

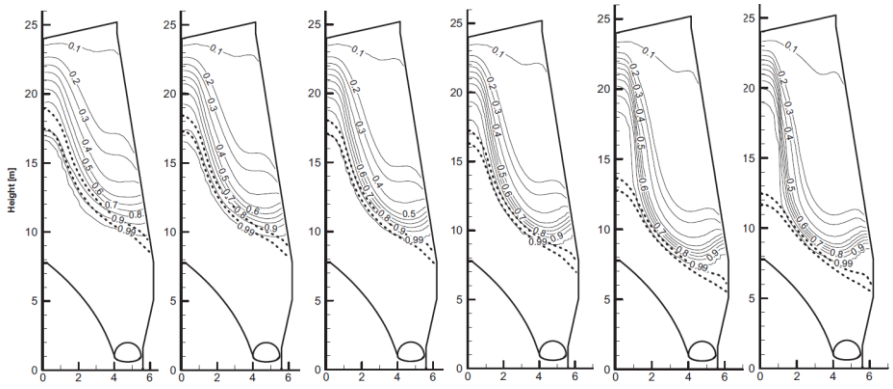

Figure 8. Distribution of reduction degree of iron bearing burden (kmol·m^3·s^{-1}). Oxygen content: (a) 24%; (b) 29.02%; (c) 35.16%; (d) 46.14%; (e) 65.01%; (f) 99.52%.[65]

It is interesting to note that in the numerical studies mentioned above, many models apply a three-interface unreacted core model of the iron oxide particles, including the one-dimensional and multi-dimensional models. However, at present, the non-stoichiometry of iron oxides has not been taken into account in the these models.[68] Therefore, the uniqueness of final product in the predominance diagram cannot be determined because the thermodynamic data does not meet the thermodynamic restrictions.[69,70]

3.1.5 *Regional Models*

The mathematical models of the TGR-OBF discussed above are, despite the growing complexity when more spatial dimensions are included, still limited by certain assumptions (e.g., symmetry, steady-state) and therefore unable to describe the regional behavior in the BF, such as the penetration and distribution of shaft-injected gas,[71] the dynamics of gas and solid flows under OBF conditions,[72] the dynamic adjustment of VPSA considering the changes of feeding gas composition, the coal combustion behavior [73] and the raceway formation and phenomena in the OBF. Some investigators have still pursued a description of such detailed behavior.

Natsui and researchers from his laboratory [71,72] studied the influence of shaft-injected gas on the gas and solid flows, using a hybrid Discrete Element Method - Computational Fluid Dynamics (DEM-CFD) approach. The in-furnace gas drag force was found not to be influenced by the shaft

gas injection except in the region near the auxiliary tuyeres and the horizontal gas velocity caused by the shaft gas injection was only observed up to 1 m above the injection point. Thus, shaft gas injection has little effect on the burden descent. The penetration effect in the horizontal direction was neither significant and the area occupied by the injected gas in the horizontal section approximately equaled the ratio of shaft-injected gas volume to blast volume from the bosh tuyeres.

Dong et al.[57] established a 2-D slot model of the OBF and numerically studied the solid burden distribution characteristics and shaft-injected gas (SIG) penetration behavior using a coupled DEM-CFD method. In this study, the factors influencing the SIG penetration, such as particle diameter, shaft tuyere diameter, and the specific ratio of the SIG flowrate to total gas flowrate, *X*, were evaluated. The simulation results revealed that the penetration behavior of SIG did not change significantly with particle diameter or shaft tuyere diameter. By contrast, the value of *X* proved to have a significant impact on the SIG distribution in shaft. With the increase in *X* the concentration of SIG in the central region increased considerably, which could help improve the indirect-reduction and heating conditions for the burden in this region.

Wu et al.[74] focused their study on the coal combustion behavior in the raceway region of a sectional 3-D OBF by means of CFD modelling. The simulated domain included the oxygen coal lance, blowpipe, tuyeres, raceway and coke bed. The process of pulverized coal combustion was described in four stages, i.e., coal volatilization, combustion of volatiles and oxidation and gasification of carbon residue. The combustion of coke was simulated by the Field Model[75] in which carbon solution loss and coke combustion reactions were included. The simulation results indicated that the temperature in the raceway increased significantly compared with the TBF. The high-temperature zone of the OBF was enlarged and the highest temperature could reach 4170 K, which was about 1500 K higher than in the TBF. (In practice, such conditions would lead to considerable gasification of many components, with a possibility of detrimental cycles in the furnace.) The CO_2 content in the raceway and the CO content in the coke bed also increased significantly under the OBF conditions. In addition, the coal burnout rate increased from about 81% (for the TBF) to almost 92% for the OBF.

Gao[20,76] studied the combustion behavior in the tuyeres under OBF conditions, and Zhou et al.[77] focused specifically on the coal combustion. The simulation results show that the coal burnout increased by 16% compared with the TBF. The oxygen content has an obvious effect on the burnout. At 70% oxygen content, the coal burnout is only 22%, with a decrease of 50% compared with that of the TBF. However, care should be taken in interpreting the results directly with respect to the operation of the (oxygen) blast furnace, since the phenomena in the true raceway are extremely complex and interrelated, which are factors that are difficult to consider in simplified formulations.

3.2. *Models Focused on Energy, Exergy and Emissions*

3.2.1. *Optimization of Energy Use and Emissions*

In order to minimize the energy consumption, CO_2 emissions and the running cost, Saxén and researchers from his laboratory carried out a series of numerical simulation studies of the oxygen blast furnace process in an integrated steel mill (ISM) [78-88] using a two-zone model of the OBF (see Section 3.1).

Since the minimum unit cost and minimum CO_2 emission are two conflicting objectives which cannot be minimized at the same time, Helle et al.[78,79] conducted a nonlinear single- and multi-

objective optimization of the TGR-OBF of an iron and steel complex based on Pareto optimality. Two recycling methods were studied: In Method 1, hot oxygen-enriched blast and cold recycled gas were applied, while Method 2 used cold oxygen-enriched blast and hot recycled gas. Figure 9 shows how the steel plant production rate and CO_2 stripping cost affect the minimum specific production cost of liquid steel at a fixed CO_2 capture cost (40 €/t). Method 1 yielded lower production costs for a low CO_2 stripping cost (< 25-28 €/t) while Method 2 is better for higher stripping costs.

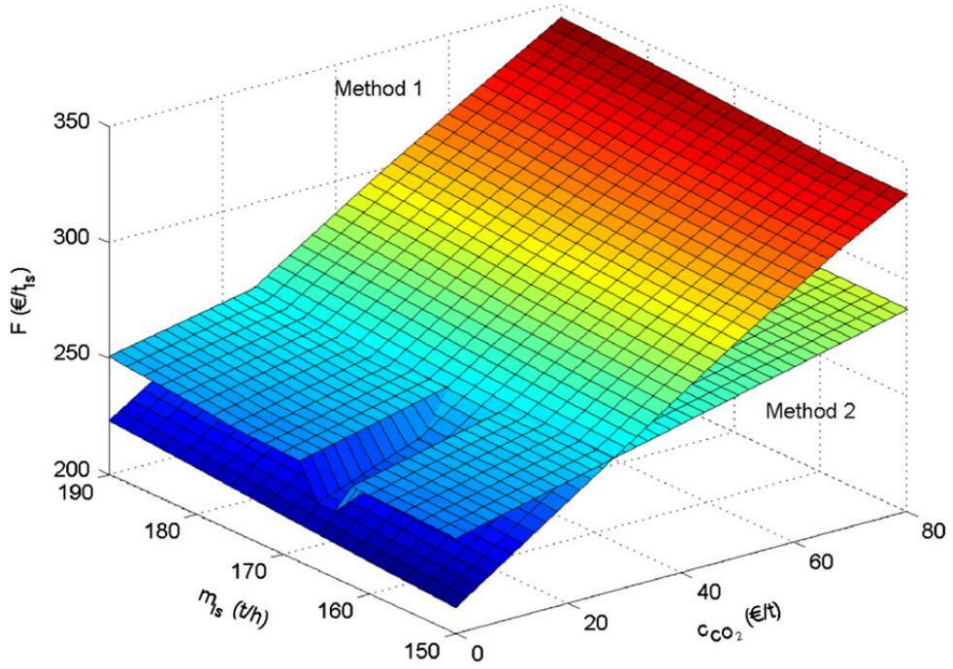

Figure 9. Minimum cost of liquid steel as function of the production rate and CO_2 emission cost for hot blast and cold recycled gas (Method 1) and hot recycled gas and cold oxygen (Method 2).[79]

Ghanbari and his co-workers[82-84] studied the oxygen blast furnace combined with a polygeneration system producing district heat, electricity and methanol in an integrated steel plant. The options studied also included the used of pre-processed biomass, which in earlier studies by the group had been demonstrated to be a feasible alternative if the price of biomass is advantageous with respect to coal and coke, and there is a sufficient penalty for CO_2 emissions.[86] Their study showed the CO_2 emissions from the system can be reduced by up to 30% by an optimal design and flexible operation of the system.

The costs and emissions of steelmaking were also studied numerically by Mitra et al.[80] for an integrated steel plant, where top gas recycling with CO_2 stripping and storage were applied. Both production costs and emissions were simultaneously minimized by a genetic algorithm. The cases with heated recycled top gas and cold injection of pure oxygen yielded as good results as the cases requiring more process units. Later, Mohanty et al.[88] proposed a *k*-optimality criterion which allows optimizing a larger number of objectives in an evolutionary framework.

An application of OBF with and without CCS (Carbon Capture and Storage) to an integrated steel plant was investigated by Arasto[89] based on the conditions of Ruukki Metals in Raahe, Finland. Implications of application of OBF to energy and mass balances at the site were studied. By applying only the OBF, the emissions can from the base level of a total emission of about 3.2 Mt/a already be reduced by 1.2 Mt/a without storing the stripped CO_2. If CO_2 is captured and stored permanently,

the emission can be reduced by an additional 1.4 Mt/a. The application of oxygen blast furnace has a significant impact not only on the coke consumption but also on the energy balance of the whole steelmaking site. In the second part of the series of studies, a correlation between the CO_2 emission cost development and electricity price development was assumed. [90] The investigators found that the economic savings depended strongly on the price of the CO_2 emission allowances.

The impact of the nature of burden and fuel on the carbon consumption and CO_2 emission of the OBF process was systematically studied by Sahu et al.[91] using a two-zone model of the furnace. They found that the total carbon requirements decreased from 420–440 to 323–342 kg/thm even for the case with a leaner-grade burden under PCI and high blast oxygen enrichment.

According to Zhang's calculation,[29] the fuel rate decreases from 496 kg/thm through 426 kg/thm to 403 kg/thm when the blast oxygen content is increased from 21.5% through 50% to 98%. Because most carbonaceous gases are deprived in the Vacuum Pressure Swing Absorption (VPSA) segment and also recycled inside of the blast furnace, the CO_2 emissions in the TGR-OBF cases decrease by 69% and 85% compared with the CO_2 emission of the conventional blast furnace process.

Jin et al.[92] also studied the energy consumption and carbon emission of an ISM with an OBF. Due to the consumption of large amount of oxygen and the removal of CO_2, an ISM with the TGR-OBF purchased 2.8 times more electricity than a conventional ISM, while the energy consumption of the ISM with the TGR-OBF was reduced to 14.4 GJ per ton crude steel. Compared with the conventional ISM, the direct CO_2 emission from the ISM with the TGR-OBF was reduced by 56% and 26% with or without CCS, respectively.

Multi-dimensional mathematical models are helpful for gaining insight into the complicated phenomena in the OBF process, but do not easily lend themselves to optimization of techno-economic indices. Hence, the optimal operating parameters of the OBF can hardly be estimated using this type of models. Despite this fact, the multi-dimensional models may be useful in finding ways to achieving efficient resource allocation with minimum expenditure. As suggested by several authors, the research on the multi-goal optimization of the OBF process could be further studied in the following two respects.

(1) The cost of CO_2 deprivation should be considered in more detail. The capture of CO_2 from the top gas mixture of different compositions should be further studied. More attention should also be paid to the CO_2 storage or utilization cost.
(2) Comparative studies between different OBF realizations should be conducted. Different oxygen contents of blast result in different and possibly completely novel inner states of the process, which will set high requirements on the process calculations to yield meaningful results.

3.2.2. *Exergy Analysis*

Exergy is the available energy, which is presented based on the second law of thermodynamics. Exergy analysis is widely used in evaluations and optimization of chemical engineering processes, including the ironmaking blast furnace.

Akiyama et al.[93] investigated the blast furnace ironmaking system integrated with methanol synthesis for reduction of carbon dioxide emission based on exergy analysis. Petela et al. [94] studied the energy and exergy consumptions of a simple system consisting of a coke oven and a blast furnace with injection of natural gas. The injection of natural gas could reduce CO_2 emission, but the energy

or exergy consumption increased. Ostrovski and Zhang[95] discussed the concept of exergy, the energy and exergy balances of blast furnaces and DIOS-type direct ironsmelting processes. They found that exergy destroyed in the blast furnace was about 5.5 GJ/thm, while exergy consumed in the direct ironsmelting is in the range of 5.0 - 9.2 GJ/thm. Direct ironsmelting processes are generally far from equilibrium in comparison with the conditions in the blast furnace. By energy and exergy analysis, Ziebik and Stanek[96] demonstrated that preheating of the blast and enrichment with a little oxygen made an improvement of the energy and exergy characteristics of the steel plant. Lampert et al.[97] presented the possibility of integration of a COREX process, a blast furnace, CO_2 removal installations and a combined heat and power plant. The exergy efficiency decreased from 0.541 to 0.505 when the CO_2 separation technology was applied in the system. Guo et al.[65] simulated the OBF operation with natural gas injection with 3-D models and exergy analysis method. When 125.4 kg/thm was injected, the coke rate and carbon emission rate decreased by 27% and 32%, respectively. The exergy efficiency decreased from about 52% to 49%. Liu et al.[98] developed an optimization model based on material and energy balances for a blast furnace, in which exergy loss was minimized. The exergy loss decreased by 5.77% and 5.14% for the minimizations of exergy loss and coke ratio, respectively.

Although a key issue in the TGR-OBF as an alternative to the TBF process is its energy and material use, very few investigators have undertaken exergy analysis of the process. Until 2017, the only systematic exergy study of the TGR-OBF with medium and full oxygen blast was the analysis presented by Zhang et al.[28] The heat exchange efficiency of the hot stoves was set as 85%, according to the practice of Bao Steel. The adiabatic combustor was fixed at 100%, and the exergy efficiency in the CO_2 deprivation stage was taken to be 90%. The operation parameters of the FOBF process are shown in Figure 2. Those of the medium oxygen enriched blast furnace (MOBF) process are a blast oxygen content of 50%, a coke rate of 300 kg/thm, a blast temperature of 1000°C, a hearth gas recycling ratio of 60%, and a hearth gas heating temperature of 1200°C. The coal rate is calculated as 126 kg/thm under the constraints of mass and heat balances. As a result, the exergy flows of the FOBF with top gas recycling are shown in Figure 10. The calculation results showed that the carbon combustion, CO_2 reduction and the second exergy consumption (defined as exergy consumption subtracted by exergy of the top gas) of the FOBF process decreased by 20%, 85% and 5% respectively, compared with the corresponding parameters of the TBF process. The analysis demonstrated that although the carbon consumption of the TGR-MOBF (case 1, Medium oxygen enriched blast furnace with top gas recycling) process decreased by 14%, this economic gain cannot offset the exergy deficit resulting from the lower output of fuel gas. In contrast, the carbon consumption in the TGR-FOBF process (case 2, Full oxygen enriched blast furnace with top gas recycling) decreased by 20%, and this profit offsets the exergy deficit resulting from the lower output of fuel gas. Another interesting result was that the thermodynamic perfection degree and exergy efficiency in both cases showed good linear relationships with the exergy efficiency of the VPSA.[28]

A similar work reported by Li[99] showed that the exergy output and the total exergy loss of the OBF-I (50% oxygen in the blast) process decreased by 1.5% and 5.6%, respectively, and those in the OBF-II (99% oxygen in the blast) process decreased by 16.6% and 30.8% compared with the TBF. However, the decrease of carbon consumption in OBF-I (6.7%) is smaller than in case 1 of the study of Zhang et al.[26] (14.1%) due to less usage of top gas in the recycling process.

Song et al.[100] calculated the energy consumption and carbon emissions of an ISM with TBF,

OBF or COREX, and made a comparison of them. Based on the operating data of the Jingtang steel plant, three steel production routes were designed and studied computationally. Compared with the conventional ISM, coking coal consumption with TGR-OBF and COREX were reduced by 39.7% and 100%. The energy consumption with the TGR-OBF was about 16% lower than in the conventional ISM and the ISM with COREX. The energy consumption of the ISM with COREX was the highest (almost 17 GJ/t-steel). This case also had the highest net CO_2 emissions, about 37% and 54% higher (International Energy Agency factor) or 32% and 28.% higher (China Grid factor) than in the conventional ISM and the ISM with TGR-OBF, respectively.

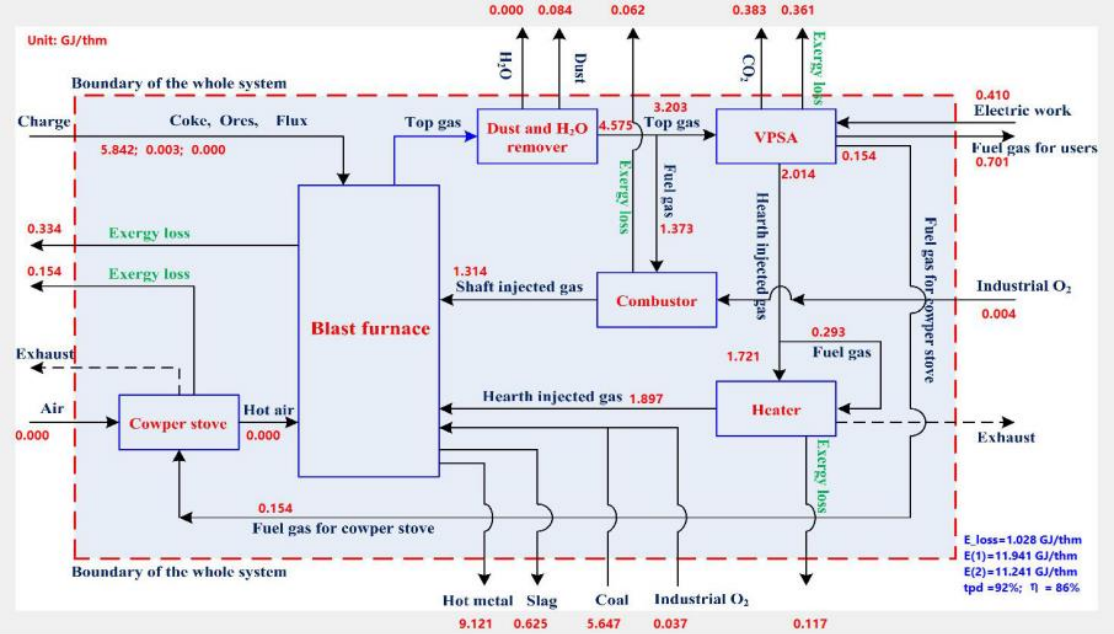

Figure 10. Exergy flows of a TGR-FOBF process[28]

3.3. *OBF Dynamics and Feasible Operation Points*

3.3.1. *Unsteady OBF Model Analysis*

Most of the literature on the TGR-OBF has been focused on the description or understanding of the steady-state of the process, but for the practical operation it is important to demonstrate the unsteady self-adaption of the compositions of the top gas and recycling gas. However, the references on the unsteady analysis of the OBF are few, especially of the unsteady process where the nitrogen decreases or accumulates with the recycles until a stable input and output is reached. In practice, such dynamic states would occur at blow-in or at sudden changes in the operating condition of the blast furnace.[101]

Since nitrogen is an inert element that does not react with any other substances in the blast furnace (ignoring NO_x formation), the unsteady evolution of the TGR-OBF process can be characterized by tracking the behavior of nitrogen. Zhang et al.[102] proposed a model to examine the accumulation of nitrogen in TGR-OBF process. If the oxygen would be pure (100%, *N_Inlet2* = 0), no nitrogen would enter with the "blast". In practice, it is not feasible to use fully pure oxygen of such quantities for economic reasons, and also other sources (PCI carrier gas, coke, etc.) introduce

nitrogen, which accumulates because of the top gas recycle. Furthermore, the combustion air of a possible shaft gas may also act as a nitrogen source. The recycling accumulation of N_2 in the OBF unsteady state is illustrated by Figure 11, where nitrogen from carrier gas, coke, coal and blast have been integrated in *N_Inlet1*. For the system inside the control volume (enclosed by the dashed line), the input of nitrogen is from the fuel materials, blast (*N_Inlet1*) and from the air used in shaft-gas combustion (*N_Inlet2*), while the output of nitrogen includes the N_2 in the export gas (*N_Outlet1*) and from the combustion tail gas of the top gas which is used as fuel to heat the recycled gas (*N_Outlet2*).

Under the condition that there is no export gas and the recycled gas injected into the hearth is heated by an external fuel (e.g., coke oven gas), we would have *N_Outlet1* = *N_Outlet2* = 0. This situation is infeasible in practice, since N_2 gradually accumulates in the system as there is only input of nitrogen.

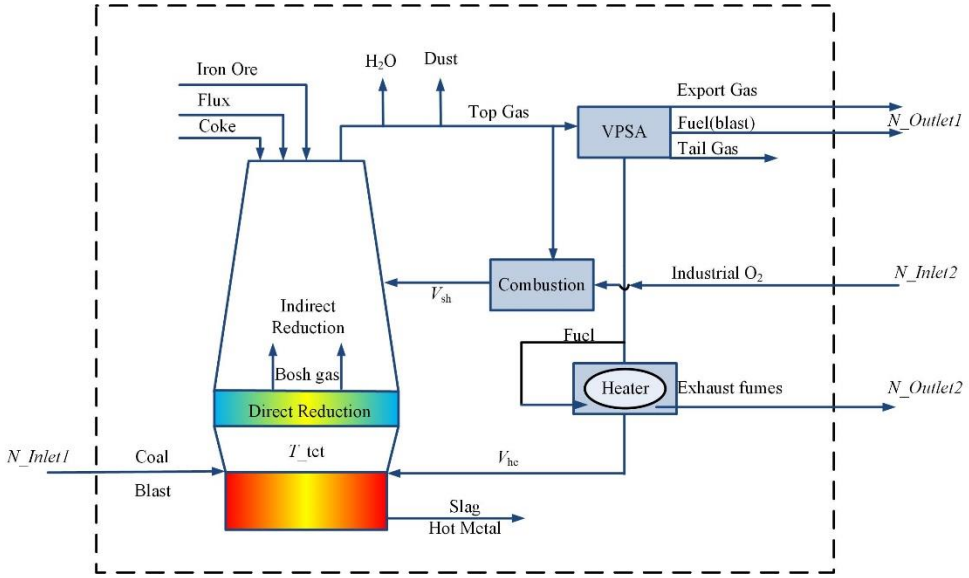

Figure 11. Nitrogen-bearing gas flow in a TGR-OBF process.[102]

For the case without export gas (*N_Outlet1*=0) but where the recycled gas is heated by the top gas, it is possible to theoretically balance the system, yielding *N_Inlet1*=*N_Outlet2*. Nevertheless, in the practical operation it is impossible to operate the system in an arbitrary steady state with only one circulation, as any fluctuations would be accumulated, leading to dynamics caused by the recycle loop. If *N_Inlet1* >*N_Outlet2* at the initial stage, the N_2 in the system will first accumulate and the calorific value of the top gas used to heat the recycled gas will decrease. As a result, the required volume of the fuel gas (considering the deprivation ratio of CO_2 to be constant) will rise in order to heat the recycled gas to the same temperature. This would make *N_Outlet2* gradually increase until *N_Outlet2*=*N_Inlet1* and hence the system reaches a balanced state. Meanwhile, the direct-reduction degree in the furnace is continuously changing until it reaches the final level. Similarly, if the change in the operational conditions of OBF makes *N_Inlet1* < *N_Outlet2*, the calorific value of top gas rises and the demand for fuel gas decreases. Meanwhile, the change in the recycled gas quantity and composition changes the direct-reduction degree in blast furnace until *N_Inlet1* = *N_Outlet2*.

When one part of the top gas after CO_2 deprivation is recycled into the shaft and hearth, and the remainder serves as fuel to heat the recycle top gas, the utilization rate of primary energy will

reach the maximum if no external gas is supplied. In general, the unsteady nature of the TGR-OBF makes it much more difficult to master this process than the conventional blast furnace.

Since the oxygen content in the blast is a critical parameter for the OBF process, recently more attention has been paid to it to compare the unsteady formulations of the FOBF process and the MOBF process. Zhang [103] established 76 equations in a quasi-unsteady mathematical model of TGR-OBF (including FOBF and MOBF) and TBF process respectively. According to the calculation results obtained, the N_2 accumulation in the system decayed to practically zero after six computational circulation loops. The evolution of the composition of the raceway gas, bosh gas and top gas are shown in Figure 12. The convergence criterion, indicating that a steady state has been reached, required the absolute difference between two consecutive values of the gas compositions to be less than 0.0005. It can be seen that the bosh gas is enriched by more CO than the raceway gas because of the direct reduction which generates CO in the bosh. The N_2 content of the top gas first accumulates and then levels off, as illustrated in the right part of Figure 12.

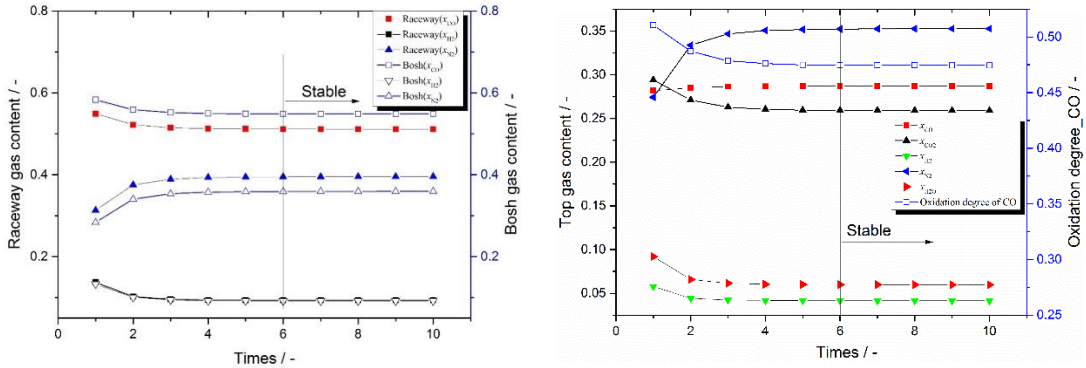

Figure 12. Evolution of the compositions of raceway gas, bosh gas and top gas in the TGR-OBF[102]

3.3.2. *Feasible and Optimal Operation State*

Although numerical analysis of the TGR-FOBF process has demonstrated that it can achieve promising economic and technical indices, the dramatic shortage of top gas in the practical operation is still an issue.[102] In order to compensate for this shortage, Zhang et al.[29] also established an model of MOBF and made a comparison between the TBF and MOBF processes operated in stable states, in order to highlight the superiority of the latter one. Under the same conditions of raw materials and fuels, the volumes of bosh gas and top gas in the TBF process were 1677 m^3/t and 1612 m^3/t respectively, with 21.5% oxygen in the blast and a blast temperature of 1200˚C. In the MOBF process, the volumes of bosh and top gas were 1432 m^3/t and 1525 m^3/t, respectively, for a blast oxygen content of 45% and blast temperature of 1000˚C. It can be seen that the volumes of bosh gas and top gas in the MOBF are 1% and 5% lower than in the TBF, while the volume of bosh gas in the FOBF usually was only 40-60% of that in TBF. This shows that the MOBF process addresses the shortage of top gas in the FOBF process.

The dependence of volumes of the top gas and bosh gas on the blast oxygen content is shown in Figure 13. It is assumed that the feasible operation regime is decided by the top gas volume, where a deviation of ±12.5% compared with that of the TBF is allowed. As a result, the top gas volume should fall in the range 1400- 1800 m^3/thm, and the feasible region of the blast oxygen content is 30-47% according to Figure 13. In this maneuverable zone, the bosh gas volume is 1100-

1500 m^3/thm, i.e., 34%-10% lower than in the TBF. Thus, one may conclude that to secure a smooth operation, the TGR-MOBF would be recommended for its low energy consumption and high productivity.

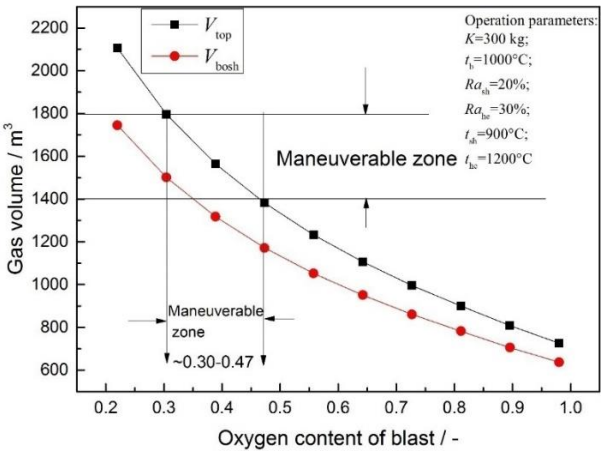

Figure 13. Volume of top gas and bosh gas *vs.* oxygen contents of blast in a MOBF[102]

Helle and Saxén [81] studied the TGR-OBF process focusing on the amount of recycled top gas and the share of it that was injected through the shaft tuyeres. They presented the feasible operation window under the given process constraints, and demonstrated the influence of different combinations of hearth and shaft gas injection on coke rate, oxygen rate and top gas composition, as well as on the CO_2 emissions. Figure 14 illustrates the results for an example where the temperature of the hot reducing gas is 1200°C, while the shaft gas temperature is 920°C. It can be seen that the limits of the operation window are set by the flame temperature and the top gas temperature constraints. The allowable specific top gas recycling rate is in the range 600-800 Nm^3/thm, and the corresponding share of shaft gas, γ, is between 0% and 48%. The coke rate is low and varies in the range 230-280 kg/thm, where the lowest value is obtained for recycled gas injection of 620 Nm^3/thm through the lower tuyeres only.

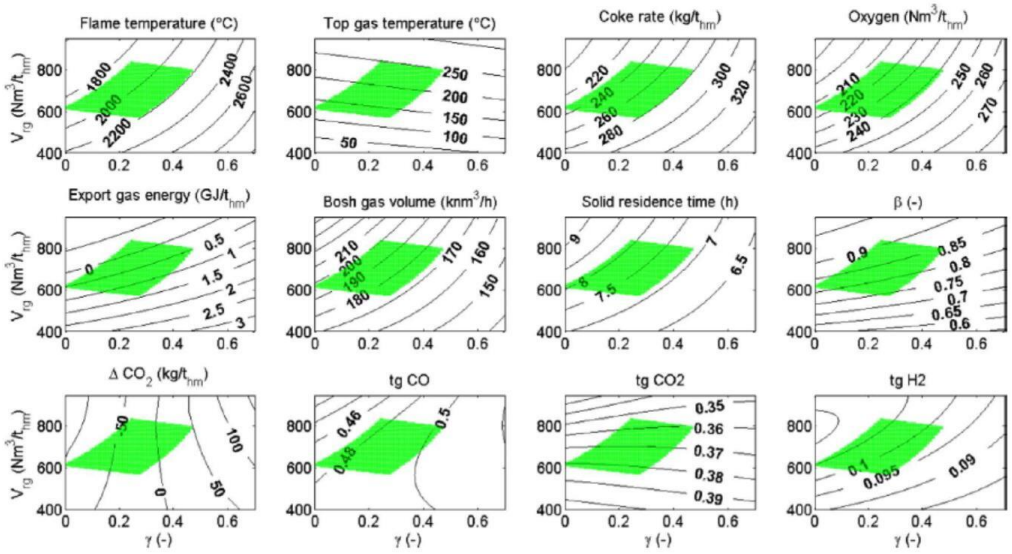

Figure 14. Feasible operation window (green area) of the TGR-OBF.[81] The subfigures depict the variables reported in the titles as functions of the share of shaft gas (γ) and the specific injected top gas rate (Nm^3/thm).

3.4. *Future Prospects for Simulation of OBF*

To summarize briefly, a comparison among these kinds of mathematical models is provided in Table 3. As shown in the table, each model type has its advantages and disadvantages. Most of the characteristics are not just limited to the studies of OBF, but are usually valid for a broad application.

Table 3 Pros and cons of different mathematical models

Model type	**Advantages**	**Disadvantages**
0-D	- Fast execution time - Small number of tunable parameters - Suitable for optimization	- Over-simplification, many fundamental assumptions - Lack of spatial information - Extrapolations may be inaccurate
1-D	- Moderate execution time - Reasonable number of parameters - Provides spatial information - Partly tunable parameters	- Convergence may be an issue - Impossible to adapt many parameters - The distributions are not 1-dimensional in the real BF: verification
2-D	- Great level of detail - Quite realistic description possible: The BF is basically 2-dimensional - Can be compared with probing results	- Long execution times - Convergence often an issue - Impossible to study sensitivity of all parameters - Inability of global optimization
3-D	- Great level of detail - Information about asymmetry - Can consider true role of raceways	- Very long execution times - Considerable numerical challenges - Detailed information obtained may be difficult to verify - Abundance of parameters - Inability of global optimization
Regional Models	- Tackle regional asymmetry - Describe unsteady process - Can capture more complicated raceway and coal combustion behavior	- Lack of global information of BF - Manual adjustment to communicate with adjacent regions - Convergence and execution time may be issues
Energy and CO_2 Emission Models	- Tackle optimization problems - Provide economical resolutions - Provide economic or environmentally friendly solutions - Multi-objective resolutions	- Usually based on simple models - Inaccuracy may result from unreasonable assumptions - Feasibility of solution needs to be proved by more complex models - Unavailable energy included
Exergy Analysis Models	- Available energy optimization - Provide economical resolutions - Provide multi-objective resolutions - Can describe the exergy indices of entity, including ancillary processes.	- Usually based on simple models - Inaccuracy may result from unreasonable assumptions - Feasibility needs to be proved by more complex models
Unsteady Models	- Provide dynamic behavior - Evolution of partial parameters - Helpful for operation of blow-in or at sudden changes	- Lack of particular regional details - Inability of global optimization - Lack of spatial detail, problems in validation
Feasible and Optimal Operation Models	- Solve feasible operation windows - Restrictive optimization considering practical issues - Can be combined with energy/exergy optimization models	- Lack of spatial information - Lack of unsteady evolution - Lack of particular regional details

As the launch of industrial trials is costly, the development of mathematical models has been playing a very important role in the process design and performance prediction of the oxygen blast furnace. In the preceding sections, we classified the mathematical models into four categories. The overall or two-zone models are the simplest ones and can be used in preliminarily studies of the comprehensive characteristics of different processes. They have also been used successfully in optimization and feasibility studies, where the best states or regions of feasible states have been determined. The 1-D, 2-D and 3-D models, which consider physicochemical details, aim at providing more accurate descriptions and deeper understanding of the in-furnace processes. These models can reveal fundamental problems that the models in the first category oversee, but the verification of the multi-dimensional models is still a challenging issue due to lack of data from the real operation. Finally, the remaining category of models focused on energy and exergy use, as well as emissions.

The simple models are important for providing overall information of the OBF that can be used as the more complicated models are applied. Moderate revisions are necessary to adapt TBF models to OBF operation. After the first one-dimensional model of the BF process had been established by Muchi[104] in the mid 1960s, the numerical descriptions of the BF process have evolved and improved dramatically.[105] Today, thanks to the rapid development of computing technology, state-of-the-art models can capture multi-dimensional and unsteady features of the BF process. Studies with such detailed models for sustainable process design are thus encouraged to find ways of substantially reducing the energy use and CO_2 emission in iron- and steelmaking. Models that to a greater extent consider practical aspects of the operation, including changing of set points and control, are clearly more complicated issues. The development of models for this purpose will be more important along with the launching of large-scale industrial trials of the OBF technology.

Based on the above survey, some potential directions of research can be identified. In the OBF blow-in practice, unsteady analysis and dynamics should be considered, including in-furnace kinetics, changes in top gas composition and volume, CO_2 depriving dynamics, and top gas recycling control. When the OBF runs steadily, it will be necessary to determine new rules of operation, e.g., to bring the furnace into a new steady-state or to recover from disturbances. Numerical simulations are expected to be helpful to assess such rules in advance in order to detect efficient strategies and to avoid unwanted states. Specifically, the influence of high productivity, high ore-to-coke ratio, and the distribution of the recycle gas should be analyzed.

4. OBF Experimental Research

4.1. *Laboratory Experiments of OBF Conditions*

4.1.1. *Implications of Thermal and Chemical Conditions in the OBF*

Under the operational conditions of OBF, the gas from raceway has a strong reducibility because of its high contents of CO and H_2. Therefore, the chemical reactions of this reductive gas with the iron oxides in the burden have become a hot topic in laboratory studies of the OBF.

Zhang[12] conducted experimental reduction experiments related to the conditions in the OBF process and the results suggested that the reduction atmosphere in the bosh evidently raised the reduction degree of the burden in the shaft. Consequently, the residence time of the burden in the blast furnace was shortened and the productivity was improved. The results of droplet tests also suggested that the reflowing temperature of iron ore increased significantly. The reflowing

temperature range was narrowed and the corresponding pressure-loss coefficient decreased, so the cohesive zone would become lower and narrower, or even disappear.

Yin et al.[106] used a Borist Furnace to mimic the reduction process in the shaft of the blast furnace with low pulverized coal injection or oxygen enriched blast, or both oxygen enriched blast and pulverized coal injection, respectively. Zuo et al.[107] studied the impact of reducing gas (H_2 and CO) on the reduction behavior of pellets in the TGR-OBF process, while Xue et al.[108] conducted a series of sinter reduction experiments in OBF atmosphere using the thermal balance weight loss method. The changes in reduction degree and reduction rate were investigated and the sinter reduction dynamics was also analyzed.

Qiao et al.[109] used a multi-region mathematical model to determine the gas composition in different regions of the OBF. The reduction processes of the burden in the OBF and TBF were also studied by applying programmed reduction devices in combination with a specific heating system. The results showed that in the OBF process, the temperatures at which the reduction of sinter and pellets started was 60°C and 150°C, respectively, lower than the corresponding temperatures in the TBF process. When the burden temperature reached 1100°C, the reduction degrees of sinter and pellets in the OBF process could reach 100% while those in the TBF process were 94% and 83%, respectively.

Li et al.[110] studied the effects of the composition and temperature of bosh gas and the water-gas reaction on the rate-limiting step of direct-reduction from wüstite (Fe_xO) to metallic iron (Fe) after the hydrogen-enriched fuel was injected into the OBF. The results suggested that the reduction potential of the bosh gas was limited under the conditions of low oxygen-enriched blast and high pulverized coal injection rate. The reduction degree of Fe_xO was only 53.6% after 90 minutes at 1000°C. An increase in the oxygen content of the blast and in the natural gas injection could lead to conditions where Fe_xO was fully reduced after 65 minutes. The gas had an even stronger reduction potential under the condition of full oxygen blast.

Chen et al.[111] focused on the cohesive zone of the OBF and studied the interactions between lump ore and sinter under the simulated conditions. The results revealed that in the OBF atmosphere, the softening and melting properties of lump ore are improved compared with those in the TBF, since the increase in the reduction degree increased the iron phase in the burden and decreased the quantity of slag phase with low melting temperature.

Wang et al.[112] studied the holdup of liquid slag in a simulated packed coke bed under OBF conditions. According to their experiment, an increasing amount of unburnt pulverized coal resulted in a significant increase of the static holdup. Flooding analysis was applied to determine the maximum static holdup, which was found to be 11.5%. It was inferred that the burnout rates of pulverized coal should exceed 79% and 84% in the traditional and oxygen blast furnaces, respectively. Thus, the OBF imposes more strict requirements on the complete combustion of the coal, which has implications for the required conditions in the raceways.

The reduction of iron ore and the degradation of coke were investigated by Wang et al.[113,114] under OBF atmosphere, especially with hydrogen-enriched operation. The influence of H_2 content in H_2-CO gas mixtures on the reduction rate of wüstite was investigated at temperatures of 1100°C, 900°C and 700°C. The reduction rate in pure H_2 atmosphere was almost three times that in pure CO atmosphere. As for H_2-CO gas mixtures, it was found that the time required to reach a reduction degree of 90% was dramatically decreased with rising H_2 content, if the H_2 content was less than 50%. For conditions where the H_2 content exceeded 50%, the influence on the reduction time was

lesser. Wang et al. suggested that a proper H_2 concentration in the bosh gas should be 20-40% to achieve a good H_2 utilization. The authors also found that with increasing ore to coke ratio, the solution loss reaction of coke was enhanced while the reduction rate of sinter tended to decrease slightly. Under the atmosphere of FOBF, the reduction degree of sinter was found to be no less than 91% after 180 min in 1000°C and the solution-loss ratio of coke was 3.7%. Under TBF atmosphere, the corresponding reduction degree was 54.3%, suggesting that the sinter needs to be further reduced in the high temperature zone of the traditional blast furnace.

4.1.2. *Pulverized Coal Combustion*

In the OBF, the quantity of pulverized coal may exceed the quantity of coke, and thus coal becomes the main energy resource. Therefore, the combustion of the pulverized coal in the OBF is an important issue.

Chai et al.[115] experimentally investigated the combustion rate of pulverized coal injected into the OBF through an improved device, as shown in Figure 15, based on the previous work conducted by Senk et al.[116] In the experimental process, a furnace at 1200°C was used to preheat the gas, simulating the hot-air supply system, while the furnace at 1500°C simulated the combustion zone of the tuyere-raceway system. First, the pulverized coal is quickly carried by high-pressure gas to the junction of the high-pressure and low-pressure parts to simulate the coal injection process of the blast furnace. Then the coal starts burning and finally the combustion process is completed in the furnace which is kept at 1500°C. The results indicated that different types of pulverized coal showed different combustibility. When the coal injection ratio was such that it would correspond to a specific injection rate of 350 kg/thm, the combustion degree varied from 46% to 79% for the different pulverized coal types. As the relative amount of oxygen to coal increased for the same type of pulverized coal, the combustion conditions improved and the combustion degree increased. Furthermore, the results also indicated that both the combustion degree and the corresponding PCR would increase with increasing coal volatiles, under the conditions of high temperature and rapid combustion. However, in the opinion of the authors of the present paper, even though the coal combustion abilities are enhanced, it does not necessarily mean that the corresponding PCR could be increased in the OBF because the productivity of hot metal was not measured in the study.

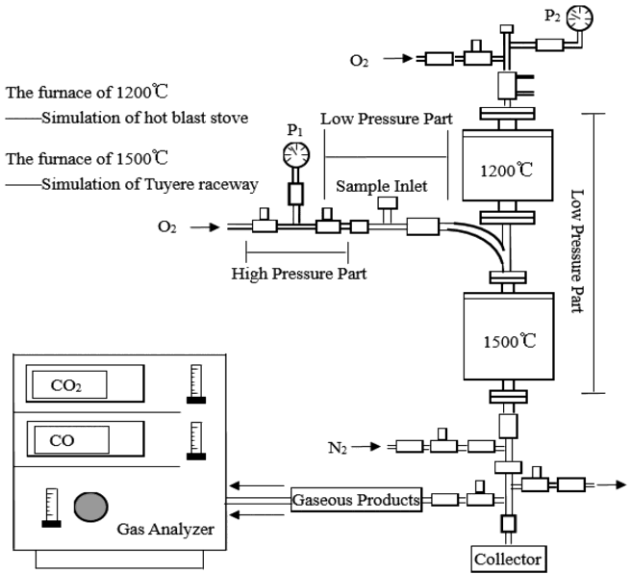

Figure 15. Schematic diagram of the equipment for the combustion of pulverized coal in blast furnace [115]

Li et al.[73] conducted an orthogonal experiment to investigate the influence of some operation parameters in the OBF process on the burnout rate of pulverized coal injected with oxygen-enriched air. Furthermore, these parameters were also analyzed in order to achieve a maximum burnout rate. Based on the experimental results, it was concluded that the order of significance of the parameters studied was 1) pulverized coal type, 2) coal injection ratio, 3) oxygen enrichment, 4) blast temperature, 5) spray gun type, 6) blast volume and 7) angle between the spray gun and the straight tube. The best combination of these operation parameters was also determined. Under optimal condition, the burnout rate was estimated to 91.4%, which was more than double that of the standard conditions. Since the range of oxygen enrichment studied was 1.5%-5.0%, this coal combustion process could not be regarded to correspond to the one in the OBF, but the work still provides valuable information and guidance for the research or design of the coal injection system and the experiments could possibly be extended to OBF-like conditions.

4.2. Pilot and Industrial OBF Experiments

4.2.1. *Industrial Trials at NKK*

After a long period of research, the Japanese steel company Nippon Kokan KK presented the NKK-OBF process in 1987, illustrated schematically in Figure 16. These two schematic figures were drawn according to the provided data of tables in the literature.[6,7] Two rows of tuyeres were arranged at the upper hearth and middle of the shaft, respectively, for the injection. Room temperature oxygen and a large amount of pulverized coal were injected in the hearth tuyeres, together with a certain volume of top gas without CO_2 deprivation to control the flame temperature. Furthermore, another proportion of the recycled top gas, which was preheated to the range 500°C-1200°C by partial combustion with oxygen, was blown into the middle shaft for gas supplement and burden preheating. In this process, the remaining top gas was exported for other utilization.

The experimental results (Table 4) of NKK-OBF process showed that the amount of coal injected could be increased to 320 kg/thm, so the corresponding coke rate decreased dramatically. Meanwhile, the pig iron output increased from 9.9 t/d to 20.0 t/d, the utilization coefficient of the BF was improved to 5.08 t/(m^3·d), and the silicon content in hot metal also decreased clearly. Based on an analysis of the experimental data, it was deemed possible to decrease the total fuel rate to 530 kg/thm if this process was put into practice. This was among the first industrial demonstrations of the feasibility of the blast furnace process with full oxygen blast.

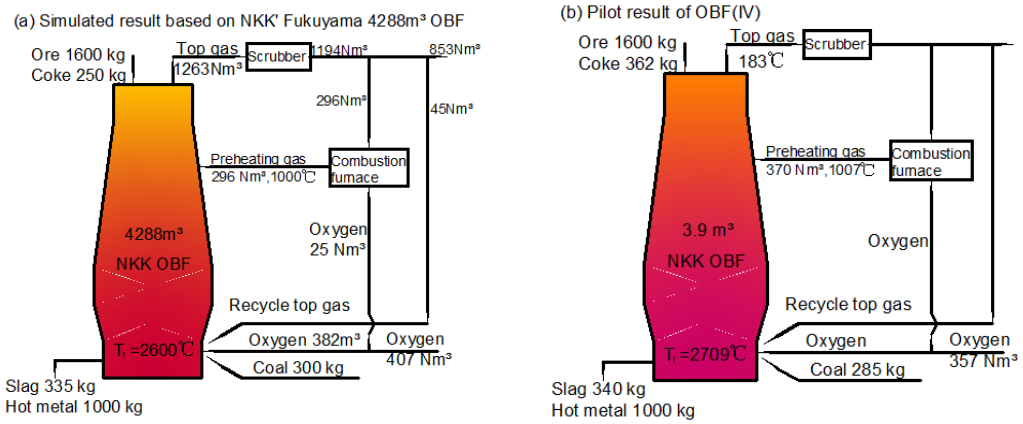

Figure 16. Outline of NKK-OBF process

Table 4. Experimental results of NKK oxygen blast furnace [7]

Stages	I	II	III	IV
	TBF	OBF	OBF	OBF
Productivity (t/d)	9.9	10.7	12.0	20.0
Coke rate (kg/thm)	688	800	352	362
Coal rate (kg/thm)	0	0	320	285
Fuel rate (kg/thm)	688	800	672	647
Blast volume (Nm^3/thm)	1530	—	—	—
Blast temp. (°C)	885	—	—	—
O_2 rate (Nm^3/thm)	39	450	383	357
Steam rate (kg/thm)	—	190	0	0
Flame temp. (°C)	2381	2705	2864	2839
Preheating rate (Nm^3/thm)	—	670	530	370
Preheating gas temp. (°C)	—	1019	988	1007
Top gas CO/CO_2(–)	1.38	1.41	1.10	1.14
Top gas temp. (°C)	257	187	226	183
Hot metal temp. (°C)	1460	1409	1418	1448
Slag rate (kg/thm)	324	362	345	340
Direct-reduction degree (–)	0.50	0.06	0.19	0.27

4.2.2. *Industrial Trials at Tula*

The Tula-OBF process was reported in 1985 by RPA Toulachermet,[9,117] a steel company of the former Soviet Union, with a process flow sheet shown in Figure 17. It is noteworthy that only one row of tuyeres was arranged at the hearth, where oxygen at room temperature and preheated reducing gas were injected. This reducing gas was taken from the top gas and preheated in a hot stove after dust removal and CO_2 deprivation. Furthermore, the system could provide export gas. The main equipment of this process included the blast furnace, dust-extraction unit, compressor, CO_2 removal unit, hot stove and oxygen generator.

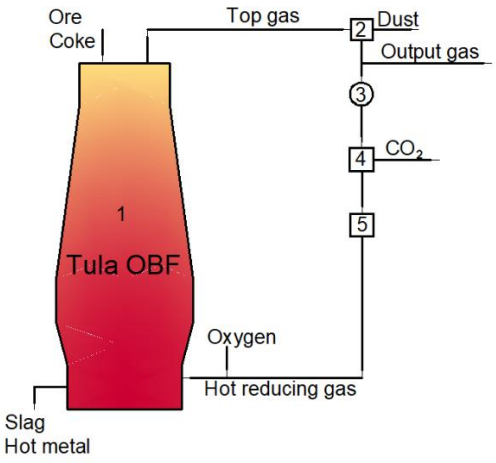

Figure 17. Flow chart of Tula OBF process. [22] 1. Blast furnace; 2. Dust collector; 3. Compressor; 4. CO_2 removal unit; 5. Hot stove

During the period 1985-1990, Tula transformed its No. 2 blast furnace (1033 m^3) into the Tula-OBF, and conducted a series of long-term trials. It was operated with full oxygen blast and hot reducing gas synchronously. The trials were conducted thirteen times with 250,000 ton hot metal produced in total with the primary goal to reduce the coke rate. According to the trial results (Table 5), the coke rate could be decrease to 367 kg/thm, the corresponding oxygen consumption was 251 Nm^3/thm, and the hot metal output was 1700 t/d. The direct-reduction degree decreased substantially, from 43.7% in the reference period to 8-9% in the experimental period. In addition, the carbon input from coke in the experimental period decreased by 28-30% compared with that in the reference period, but the overall carbon input to the BF increased by 25-35%. Until 2020, this was still the largest industrial OBF trial in history.

Table 5. Experimental results of Tula oxygen blast furnace [9]

Item	Designed	1987	1987	1988	1988
	Index	TBF	OBF	TBF	OBF
Productivity (t/d)	1800	1101	1238	1067	1702
Coke rate (kg/thm)	353	538	468	606	367
Hot reducing gas rate (Nm^3/h)	76500	40	52000	2060	47600
Hot reducing gas volume (Nm^3/thm)	1020	0.9	1008	46	671
Hot reducing gas temp. (°C)	1200	876	1120	1014	1105
O_2 content of hot reducing gas (%)	0	0	3.2	0	5.8
O_2 rate (Nm^3/h)	18400	81	20100	87.7	17800
Specific O_2 enrichment (Nm^3/thm)	245	1.766	390	1.973	251
O_2 content of blast (%)	95	21.8	69.5	23	87.2
Flame temp. (°C)	2160	2060	1870	2100	1950

In the practical operation of the FOBF, some of the process parameters deteriorated. In the industrial trials of Tula-OBF, the drainage ability of the hearth deteriorated after the furnace was ran for a long period with low coke consumption and low velocity of the oxygen blast, which reduced the extent of the raceway zones and led to frequent shutdowns.[9] In the experiments of the FOBF process, the solid flow pattern was dramatically influenced by the gas flowrate in the furnace.[118,119] Therefore, bosh or top gas shortage may occur, as mentioned in the subsection 3.2.2., which might result in hangings and slips, and other disturbances requiring a shutdown of the furnace.[9]

4.2.3. *Experimental Trials of ULCOS*

In 2004, the Ultra-low CO_2 Steelmaking (ULCOS) project was started in Europe. This project aimed to reduce the CO_2 emissions from the steelmaking sector by 50% and proposed the TGR-OBF as one of the promising alternative ironmaking processes. In 2007, the project team of ULCOS conducted a series of experiments in the experimental blast furnace of LKAB in Sweden with recycling gas injection into the hearth and shaft. These experiments studied three different concepts and lasted for seven weeks.[120] The flow chart of the different processes is shown in Figure 18.

The experimental blast furnace has a working volume of 9 m^3, shaft diameter of 1.4 m, throat diameter of 1.0 m, working height of 6.0 m, a maximum top pressure of 1.5 bar, three tuyeres with

a diameter of 54 mm. With recycled gas of 1250°C injected into the hearth, the experimental results indicated that coke and coal rates of 360 kg/thm and 140 kg/thm, respectively, could be reached at stable operation. The injection volume of the recycled gas was around 650 Nm^3/thm. In the process concept where the recycled gas was injected both into the hearth and shaft, the coke and coal rates were 260 kg/thm and 170 kg/thm, respectively. The volumes of the gas injected into hearth and shaft were both 550 Nm^3/thm.

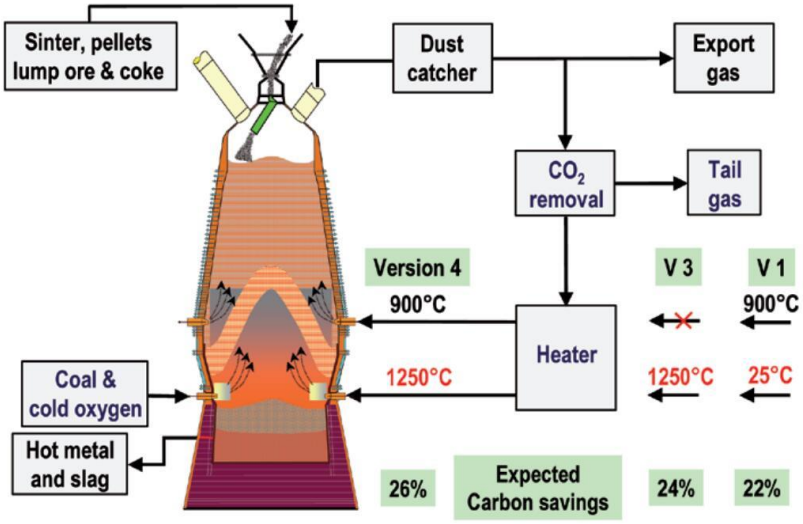

Figure 18. Flow chart of TGR-OBF process of ULCOS[120]

4.2.4. *Industrial Trials of Yingkou*

In June 2009, the State Key Laboratory of Advanced Steel Processes and Products of China (Beijing) in cooperation with Minmetals Yingkou Medium Plate conducted semi-industrial trials of an experimental blast furnace with a working volume of 8 m^3.[121] This is generally regarded as the first step of development of the Chinese OBF process.[122] In this system, rows of tuyeres were arranged at the hearth and shaft. Room temperature oxygen and pulverized coal were injected into the hearth tuyeres while preheated COG (900°C) was blown into the shaft tuyeres.

The experiments were conducted in three stages as shown in Table 6. The first stage proceeded for 15 days with hot metal produced smoothly at a coke rate of 872 kg/thm and a coal rate of 316 kg/thm. The second stage lasted for 23 days, aiming to resolve the problems regarding to the cooling of the injection devices and to eliminate hangings in the furnace. The coke rate and coal rate approached to 583 kg/thm and 450 kg/thm, respectively. Finally, the third stage lasted for 18 days, with the goal to investigate various operation indices of the OBF with coke oven gas injected into the shaft. As the flowrate of COG was 180 Nm^3/thm, the coke rate and coal rate could be decrease to 497 kg/thm and 403 kg/thm, respectively, which met the expected target. The top gas carbon monoxide utilization ratios, $\eta_{CO} = x_{CO_2}/(x_{CO} + x_{CO_2})$ in the three stages were 18.8%, 22.3% and 25.9%, respectively. The high fuel rate of the Yingkou OBF trial was a result of the low utilization of CO. If the top gas were recycled, the fuel rate would decrease dramatically. This campaign should be seen as a preparatory step for conducting OBF industrial trials in China.

Table 6 Experimental results of oxygen blast furnace in Yingkou [121]

Item		I	II	III
Productivity (t/h)		1.8	2.2	2.7
Coke rate (kg/thm)		872	583	497
Coal rate (kg/thm)		316	452	403
O_2 rate (Nm^3/thm)		767	633	551
COG rate (Nm^3/thm)		—	—	180
COG temp. (°C)		—	—	900
Hot metal temp. (°C)		1473	1456	1438
Hot metal composition (%)	C	4.5	4.3	4.2
	Si	2.8	2.2	1.8
	Mn	0.29	0.24	0.26
	P	0.123	0.115	0.138
	S	0.064	0.043	0.059
Slag basicity, CaO/SiO_2(–)		1.12	1.09	1.16
FeO in slag (%)		1.25	1.68	1.52
Top gas η_{CO}		18.8	22.3	25.9
Top gas temp. (°C)		286	264	326
Utilization coefficient ($t/m^3 \cdot d$)		5.4	6.6	8.1

4.2.5. *Industrial Trials of COURSE 50*

COURSE 50[123] was a large Japanese project aiming at an environmentally-friendly steelmaking process. It was carried out by Kobe Steel and other five cooperative companies, and was commissioned by the New Energy and Industrial Technology Development Organization. COURSE 50 focused on developing a process of OBF combined with COG injection to reduce CO_2 emissions in steelmaking.

During the period from April to November in 2013, the project team of COURSE 50 conducted semi-industrial trials regarding COG and regraded coke oven gas (RCOG) injection into the OBF using the experimental blast furnace of LKAB in Sweden.[124] By injecting 99 kg/thm of COG (57% H_2, 31.3% CH_4, 11.7% N_2) into blast enriched by 7.8% oxygen at a pulverized coal rate of 123 kg/thm, a coke rate of 432 kg/thm was achieved. The blast temperature could here be lowered to 982°C. Injecting 149 kg/thm of RCOG (77.9% H_2, 10% CO and 12.1% N_2) into blast enriched by 6.9% oxygen at a pulverized coal rate of 128 kg/thm, a coke rate of 435 kg/thm was reached at a blast temperature of 972°C. Thus, the two operation states are very similar with respect to the resources used.

The most effective way to reduce greenhouse gas emission is to substitute carbonaceous reducing gas by hydrogen-enrich gas, but it is not economically feasible at present due to the high cost of hydrogen production. However, from research and development perspectives, it is motivated to study any promising means of suppressing emissions to avoid the negative consequences of climate change.

4.2.6 Industrial Trials of Baowu Group

In mid July 2020, an OBF with an inner volume of 430 m^3 was blown in at Xinjiang Bayi Steel,

Baowu group.[125] This OBF was adapted from a small industrial blast furnace of the company. The first campaign is divided into two stages. The first stage will last 3-4 months with an aim to reach an oxygen content of 35% in the blast, which is at the upper feasibility end of TBF operations. In the second stage, also planned to last 3-4 months, top gas recycling will be applied with CCS, achieving an oxygen content of 50% in the blast. The goal is to explore industrial operation of the TGR-MOBF concept. Finally, operation under hydrogen-enriched gas supply will be studied.

Before the industrial trial, Li et al.[126] from Xinjiang Baiyi Steel calculated the theoretical energy consumption of the OBF. As shown in Table 7 (where "kg ce" denotes the China national standard of energy consumption based on the combustion heat of 1 kg standard coke), although the oxygen requires more energy, the savings of coke offset this negative influence and result in an advantage in the energy demand compared with that of the TBF process. The Baowu effort is the first industrial-scale industrial OBF trial in China, and the second largest OBF trial globally thus far.

Table 7 Designed parameters of the Baowu 430 m^3 OBF compared with that of TBF[126]

Item	430 m^3 TBF			430 m^3 OBF		
	Demand (thm^{-1})	Coefficient	Energy (kg ce)	Demand (thm^{-1})	Coefficient	Energy (kg ce)
Electricity	72 kWh	0.123 kg ce/kWh	8.85	68 kWh	0.123 kg ce/kWh	8.36
N_2	21.0 m^3	0.370 kg ce/ m^3	7.77	21.00 m^3	0.370 kg ce/ m^3	7.77
O_2	32.4 m^3	0.400 kg ce/ m^3	12.95	274.42 m^3	0.400 kg ce/ m^3	109.77
Blast	1295 m^3	0.088 kg ce/ m^3	113.97	-	-	-
CO_2 removal	-	-	-	800 m^3	0.023 kg ce/ m^3	18.11
Coal	143 kg	0.900 kg ce/ kg	128.70	150.00 kg	0.900 kg ce/ kg	135.00
Coke	432 kg	0.971 kg ce/ kg	419.64	289.00 kg	0.971 kg ce/ kg	280.73
Top gas	-1124 m^3	0.129 kg ce/ m^3	-144.51	-181.43 m^3	0.257 kg ce/ m^3	-46.66
Total			547.37			513.07

4.3. *Future Prospects for Experimental OBF Studies*

The experimental studies focusing on pulverized coal combustion and solid burden reduction in the atmosphere of the OBF have yielded a better understanding of the complicated inner physicochemical processes of the process. Furthermore, the experimental findings also play important roles as references in evaluating the results obtained from corresponding numerical models.

The semi-industrial and full-scale OBF trials showed different degrees of success, but have proved that the practical operation of the OBF is possible. Nevertheless, at present the OBF process is still not very competitive in terms of economy and operation stability compared with the TBF process. Some problems, such as intermittent unsmooth operation (with channeling, hangings and slips) appeared in the experiments and the costs were quite high. For example, in the Tula trials, although the carbon input from coke decreased by about 30% compared with that in the reference period, the overall carbon input still increased by 25-35%. The hearth drainage ability also deteriorated gradually. Therefore, in order to compensate for these drawbacks of the FOBF process, more experimental work on the MOBF process is strongly recommended based on the findings of simulation studies.[102]

Finally, it should be noted that the TBF process has been developed for more than 200 years, while the OBF process only for about 50 years, with little activities in the 1990s and first years of the present century. Therefore, many potential difficulties in the OBF as well as in the auxiliary systems, such as top gas heating and CO_2 capture technology [127-131] must be solved in the future. It is essential to pay due attention to solving both theoretical and practical difficulties of the OBF process in order to reach long-term benefits, including suppressing CO_2 emissions and enhancing the productivity and material and energy efficiency of the ironmaking process.

5. Conclusions and Future Perspectives

A large number of numerical and experimental studies conducted to investigate and develop the OBF process have been introduced and reviewed in this paper. Based on the different OBF techniques proposed and evaluated, some comments and perspectives were summarized:

(1) The direct-reduction degree and thermal reserve zone temperature should be selected or calculated appropriately in simple zonal models of the OBF to obtain reliable results. The changes in productivity, heat loss and the upper limit of pulverized coal injection should also be taken into account more accurately in OBF studies with this category of numerical models.

(2) The non-stoichiometry of ferric oxides should be noted when considering gas-solid reduction reactions in detailed mathematical models and the thermodynamic data used should meet the thermodynamic constraints. For the multi-goal optimized models, the cost of CO_2 deprivation should be considered in more detail (e.g., varying with the CO_2 content of the top gas). Optimization of the OBF processes with different oxygen enrichments and recycling concepts (hearth and shaft tuyeres) should be also addressed.

(3) At present, the FOBF process cannot still compete with the TBF process in terms of smoothness of operation. This is partly due to the complicated and non-linear behavior of the feedback induced by the top gas recycle. For instance, a change in the reduction rates will be reflected in the top gas composition, which will affect the tuyere conditions, etc. Furthermore, as the process is operated with less coke, i.e., lower coke reserve, control of the OBF is expected to be much more challenging. Likewise, the operation of the hearth at high productivity and low coke rates is expected to be problematic. For the reduction of CO_2 emission and sustainable development in the long run, more efforts and intensive research are required to tackle these issues.

(4) The MOBF process with top gas recycling is a promising variant of the OBF process due to its low energy consumption and stable operation. Although higher profit is expected in the FOBF process, the MOBF process should be superior in terms of smooth operation and feasibility, and is therefore recommended as a forerunner. Along with experienced gathered in operating the MOBF, the oxygen content of the blast can be gradually increased towards FOBF conditions.

Nomenclature

Roman Letters	
K	Coke rate (kg/thm)
N_Inlet1	Nitrogen carried by coal and blast (Nm^3/thm)
N_Inlet2	Nitrogen carried by industrial O_2 used in the shaft (Nm^3/thm)
$N\_Outlet1$	Nitrogen carried by top gas for both export and fuel usage (Nm^3/thm)
$N\_Outlet2$	Nitrogen carried by heat-supporting top gas in the hearth recycle (Nm^3/thm)
Q_{in}	Total heat input of blast furnace (MJ/thm)
Q_{out}	Total heat output of blast furnace (MJ/thm)
Ra_{he}	Share of hearth recycled gas to top gas after VPSA
Ra_{sh}	Share of shaft recycled gas to top gas
R_d	Direct-reduction degree
T_b, t_b	Temperature of preheated gas (℃)
t_{he}	Temperature of hearth injected gas
T_R	Temperature of thermal reserve (℃)
t_{sh}	Temperature of shaft injected gas
T_{TCT}	Theoretical combustion temperature (℃)
V_b	Blast Volume (Nm^3/thm)
V_{bosh}	Volume of bosh gas (Nm^3/thm)
V_{he}	Total volume of the hearth injected gas (Nm^3/thm)
V_{rg}	Volume of recycled gas after CO_2 stripping (Nm^3/thm)
V_{sh}	Total volume of the shaft injected gas (Nm^3/thm)
V_{top}	Volume of top gas (Nm^3/thm)
X	Ratio of the SIG flowrate to total gas flowrate
x_i	Volume fraction of gas i (i = CO, CO_2, H_2, N_2, etc.)
Greek Letters	
β	Share of top gas recycled
γ	Share of shaft gas
ξ	Oxygen-to-carbon ratio

Abbreviations

BF	Blast furnace
BOBF	Balanced oxygen blast furnace
CCS	Carbon capture and storage
COG	Coke oven gas
FOBF	Full oxygen blast furnace
FRG	Flowrate of recycled gas, Nm^3/thm
ISM	integrated steel mill
LGC	Less-gas-circulation
MOBF	Medium oxygen enriched blast furnace
OCF	Oxygen-Coal-Flux
PCI	Pulverized coal injection
PCR	Pulverized coal rate
RCOG	Regraded coke oven gas
SIG	Shaft-injected gas
TBF	Traditional blast furnace
Temp.	Temperature
TGR-FOBF	Full oxygen enriched blast furnace with top gas recycling
TGR-MOBF	Medium oxygen enriched blast furnace with top gas recycling
TGR-OBF	Oxygen blast furnace with top gas recycling
VPSA	Vacuum Pressure Swing Adsorption

Acknowledgements

This research was funded by the National Natural Science Foundation of China (NSFC), grant number 51804228 and 51874214, and the China Scholarship Council, grant number 201908420169, and Postdoctoral Research Foundation of China, grant number 2020M672425.

References

[1] J. J. Cai, *World Iron & Steel* **2009**, 1.

[2] M. S. Chu, X. Z. Guo, F. M. Shen, J. Yagi, *J. Northeastern Univ. (Natural Science)* **2007**, 28, 829.

[3] J.T. Ma, *Bergsmannen med Jernkontorets Annaler* **2000**, 3, 76.

[4] T. Ariyama, J. Yagi, *ISIJ Int.* **1998**, 38, 896.

[5] H. Nogami, *ISIJ Int.* **2019**, 59, 607.

[6] Y. Ohno, M. Matsuura, H. Mitsufuji, T. Furukawa, *ISIJ Int.* **1992**, 32, 838.

[7] Y. Ohno, H. Hotta, M. Matsuura, H. Mitsufuji, H. Saito, *Tetsu-To-Hagane* **1989**, 75, 1278.

[8] H. Yamaoka, Y. Kamei, *ISIJ Int.* **1992**, 32, 701.

[9] M. A. Tseitlin, S. E. Lazutlin, G. M. Styopin, *ISIJ Int.* **1994**, 34, 570.

[10] J. O. Edström, J. T. Ma, *Scandinavian J. Metall.* **1989**, 18, 105.

[11] Y. Ohno, H. Hotta, M. Matsuura, *Trans. Iron Steel Inst. Jpn.* **1987**, 27, 219.

[12] J. L. Zhang, *Doctoral Thesis*, University of Science and Technology of Beijing **2001**.

[13] Y. Han, Q. Xue, Y. Li, *Adv. Mater. Res.* **2010**, 146-147, 417.

[14] K. Takahashi, T. Nouchi, M. Sato, T. Ariyama, *ISIJ Int.* **2015**, 55, 1866.

[15] F. Didelon, Y. Rachenne, C. Gillion, J. Borlee, D. Sert (Arcelormittal Investigación y Desarrollo, S.L., Sestao Bizkaia), US, 8992664B2, **2015**.

[16] J. Van der Stel, G. Louwerse, D. Sert, A. Hirsch, N. Eklund, M. Pettersson, *Ironmak. & Steelmak.* **2013**, 40, 483.

[17] M. Sato, K. Takahashi, T. Nouchi, T. Ariyama, *ISIJ Int.* **2015**, 55, 2105.

[18] W. Wenzel, H. W. Gudenau, T. Fukushima (Nippon Kokan Kabushiki Kaisha of Japan), US, 3884677, **1973**.

[19] F. Fink, presented at *Oxygen-Coal Iron-Steelmaking International Conference*, Beijing, June **1997**.

[20] P. Gao, *Doctoral thesis*, Northeastern University **2013**.

[21] W. K. Lu, K. R. Vasant, *ISS Trans.* **1984**, 5, 25.

[22] D. D. Yuan, *Master's Thesis*, Northeastern University **2012**.

[23] M. S. Qin, Y. H. Xie, Y. Y. Yang, N. F. Yang, F. Gu, D. N. Reng, *Iron and Steel* **1985**, 20, 13.

[24] A. Poos, N. Ponghis, presented at *Ironmaking Conference of AIME*, Detroit, March **1990**.

[25] J. T. Ma, J. O. Edström, *Scandinavian J. Metall.* **1992**, 21, 104.

[26] J. O. Edström, J. V. Schéele, *Scandinavian J. Metall.* **1993**, 22, 2.

[27] Z. K. Gao, presented at *Oxygen-Coal Iron-Steelmaking International Conference*, Beijing, June **1997**.

[28] W. Zhang, J. H. Zhang, Z. L. Xue, *Energy* **2017**, 121, 135.

[29] W. Zhang, J. H. Zhang, Z. L. Xue Z. S. Zou Y. H. Qi, *ISIJ Int.* **2016**, 56, 1358.

[30] M. S. Qin, Z. K. Gao, G. L. Wang, *Iron and Steel* **1987**, 22, 1.

[31] Y. M. Shang, Y. S. Xie, Q. Ai, H. Zhang, *Eng. Chem. & Metall.* **1993**, 14, 189.

[32] G. Danloy, J. Van der Stel, P. Schmöle, presented at *4th ULCOS seminar*, Essen, October **2008**.

[33] P. M. Guo, J. J. Gao, P. Zhao, *J. Univ. Sci. Technol. Beijing* **2011**, 33, 334.

[34] Y. H. Han, J. S. Wang, Y. Z. Li, X. F. She, L. T. Kong, Q. G. Xue, *J. Univ. Sci. Technol. Beijing* **2011**, 33, 1280.

[35] Z. L. Lei, *Master's Thesis*, Northeastern University **2014**.

[36] X. F. She, X. W. An, J. S. Wang, Q. G. Xue, L. T. Kong, *J Iron Steel Res. Int.* **2017**, 24, 608.

[37] J. L. Zhang, G. W. Wang, J. G. Shao, H. B. Zuo, *J. Iron Steel Res. Int.* **2014**, 21, 151.

[38] S. R. Na, *Ironmak.* **1983**, 1, 49.

[39] T. Miyazaki, H. Yamaoka, Y. Kamei, F. Nakamura, *Tetsu-to-Hagane* **1987**, 73, 2122.

[40] M. Matsuura, H. Mitsufuji, T. Furukawa, Y. Ohno, presented at *6th International Iron and Steel Congress*, Nagoya, January **1990**.

[41] M. S. Qin, Y. T. Zhang, *Acta Metall. Sin.* **1987**, 23, B1.

[42] M. S. Qin, Y. T. Zhang, H. S. Lu, J. L. Zhang, *Iron and Steel* **1990**, 25, 9.

[43] X. Tang, C. S. Xu, *J. Chongqing Univ.* **1995**, 18, 109.

[44] J. Yagi, *Tetsu-to-Hagane* **1973**, 69, 1242.

[45] M. Hatano, K. Kurita, H. Yamaoka, T. Yokoi, *Tetsu-to-Hagane* **1982**, 68, 2377.

[46] X. G. Bi, *ISIJ Int.* **1992**, 32, 470.

[47] P. Jin, Z. Y. Jiang, C. Bao, Y. X. Lu, J. L. Zhang, X. X. Zhang, *Steel Res. Int.* **2016**, 87, 320.

[48] M. Kuwabara, K. Isobe, K. Mio, K. Nakanishi, I. Muchi. The joint symposium of Iron and Steel Institute of Japan and the Australasian Institute of Mining and Metallurgy. In Proceedings of 2nd Japan-Australia Symposium, Tokyo, October **1983**.

[49] H. Nishio, T. Miyashita, *Tetsu-to-Hagane* **1973**, 59, 1506.

[50] T. Yatsuzuka, K. Nakayama, K. Omori, Y. Hara, M. Iguichi, *Tran. Iron Steel Inst. Jpn*. **1973**, 13, 115.

[51] Z. L. Zhang, J. L. Meng, L. Guo, Z. C. Guo, Z.C, *Metall. Mater. Trans. B* , **2016**, 47B, 467.

[52] Z. L. Zhang, J. K. Meng, L. Guo, Z. C. Guo, *JOM*, **2015**, 67, 1936.

[53] Z. L. Zhang, J. L. Meng, L. Guo, Z. C. Guo, *JOM*, **2015**, 67, 1945.

[54] L. Z. Liu, Z. Y. Jiang, X. R. Zhang, Y. X. Lu, J. K. He, J. S. Wang, X. X. Zhang, *Energy* **2018**, 163, 144.

[55] Z. Y. Li, S. B. Kuang, A. B. Yu, J. J. Gao, Y. H. Qi, D. L. Yan, Y. T. Li, X. M. Mao, *Metall. Mater. Trans. B.* **2018,** 49, 1995.

[56] Z. Y. Li, *Doctoral Thesis*. Monash University **2017**.

[57] Z. S. Dong, J. S. Wang, H. B. Zuo, X. F. She, Q. G. Xue, *Particuology* **2017**, 32, 63.

[58] X. B. Yu, Y. S. Shen. *Metall. Mater. Trans. B* **2020**, 51, 1760.

[59] J. Yagi, *ISIJ Int.* **1993**, 33, 619.

[60] J. A. Castro, H. Nogami, J. Yagi, *ISIJ Int.* **2002**, 42, 44.

[61] P. R. Austin, H. Nogami, J. Yagi, *ISIJ Int.* **1997**, 37, 748.

[62] P. R. Austin, H. Nogami, J. Yagi, *ISIJ Int.* **1998**, 38, 239.

[63] M. Chu, *Doctoral Thesis*, Tohoku University **2004**.

[64] Y. S. Shen, B. Y. Guo, S. Chew, P. Austin, A. B. Yu, *Metall. Mater. Trans. B* **2015**, 46B, 432.

[65] T. L. Guo, M. S. Chu, Z. G. Liu, Z. Tang, J. I. Yagi, *Steel Res. Int.* **2013**, 84, 333.

[66] M. Chu, J. I. Yagi, *Steel Res. Int.* **2010**, 31, 1043.

[67] Z. Liu, M. Chu, T. L. Guo, H. Wang, X. Fu, *Ironmak. & Steelmak.*, **2016**, 43, 64.

[68] W. Zhang, J. H. Zhang, Z. S. Zou, Q. Li, Y. H. Qi, *Ironmak. & Steelmak*. **2014**, 41, 715.

[69] W. Zhang, J. H. Zhang, Q. Li, Z. S. Zou, *J. Northeastern Univ. (Natural Science)* **2013**, 34, 1430.

[70] W. Zhang, J. H. Zhang, Z. S. Zou, B. Tang, *J. Northeastern Univ. (Natural Science)* **2013**, 34, 1597.

[71] S. Natsui, S. Ueda, H. Nogami, J. Kano, R. Inoue, T. Ariyama, *ISIJ Int.* **2011**, 51, 1410.

[72] S. Natsui, S. Ueda, H. Nogami, J. Kano, R. Inoue, T. Ariyama, *ISIJ Int.* **2011**, 51, 51.

[73] Y. Q. Li, X. H. Zhang, J. X. Zhang, *App. Therm. Eng.* **2014**, 67, 72.

[74] J. M. Wu, Z. F. Zhou, X. Peng, *Nonferrous Metals Sci. Eng.* **2018**, 9, 1.

[75] M. A. Field, *Combustion of pulverized coal*, British Coal Utilization Research Association, London, **1967**.

[76] P. Gao, Q. Li, Z. S. Zou, Y. Gan, *Metal. Int*. **2013**, 18, 138.

[77] Z. F. Zhou, Q. G. Xue, H. Q. Tang, G. Wang, J. S. Wang, *JOM* **2017**, 69, 1790.

[78] H. Helle, M. Helle, F. Pettersson, H. Saxén, *ISIJ Int.* **2010**, 50, 1380.

[79] H. Helle, M. Helle, H. Saxén, *Chem. Eng. Sci.* **2011**, 66, 6470.

[80] T. Mitra, M. Helle, F. Pettersson, H. Saxén, N. Chakraborti, *Mater. Manuf. Processes* **2011**, 26, 475.

[81] M. Helle, H. Saxén, *ISIJ Int.* **2015**, 55, 2047.

[82] H. Ghanbari, F. Pettersson, H. Saxén, *Chem. Eng. Sci.* **2015**. 129, 208.

[83] H. Ghanbari, F. Pettersson, H. Saxén, *Chem. Eng. Res. Des.* **2015**, 102, 322.
[84] H. Ghanbari, M. Helle, F. Pettersson, H. Saxén, *Ind. Eng. Chem. Res.* **2011**, 50, 12103.
[85] H. Helle, *Doctoral Thesis*, Åbo Akademi University **2014**.
[86] H. Helle, M. Helle, H. Saxén, F. Pettersson, *ISIJ Int.* **2009**, 49, 1316.
[87] H. Helle, M. Helle, H. Saxén, F. Pettersson, *ISIJ Int.* **2010**, 50, 931.
[88] K. Mohanty, T. Mitra, H. Saxén, N. Chakraborti, *Steel Res. Int.* **2016**, 87, 1284.
[89] A. Arasto, E. Tsupari, J. Kärki, J. Lilja, M. Sihvonen, *Int. J. Greenh. Gas Con.* **2014**, 30, 140.
[90] E. Tsupari, J. Kärki, A. Arasto, J. Lilja, K. Kinnunen, M. Sihvonen, *Int. J. Greenh. Gas Con.* **2015**, 32, 189.
[91] R. K. Sahu, S. K. Roy, P. K. Sen, *Steel Res. Int.* **2015**, 86, 502.
[92] P. Jin, Z. Y. Jiang, C Bao, S. Y. Hao, X. X. Zhang, *Resour. Conserv. Recy.* **2017**, 117, 58.
[93] T. Akiyama, H. Sato, A. Muramatsu, J. I. Yagi, *ISIJ Int.* **1993**, 33, 1136.
[94] R. Petela , W. Hutny , J. T. Price, *Adv. Environ. Res.* **2002**, 6, 157.
[95] O. Ostrovski, G. Q. Zhang, *Energy* **2005**, 30, 2772.
[96] A. Ziebik, W. Stanek, *Int J. Energ. Res.* **2006**, 30, 203.
[97] K. Lampert, A. Ziebik, W. Stanek, *Energy* **2010**, 35, 1188.
[98] X. Liu, L. G. Chen, X. Y. Qin, F. R. Sun, *Energy* **2015**, 93, 10.
[99] C. L. Li, Q. G. Xue, Y. L. Liu, Z. S. Dong, G. Wang, J. S. Wang, *Ironmak. & Steelmak*. **2019**, 46, 761.
[100] J. Y. Song, Z. Y. Jiang, C. Bao, A. J. Xu, *Metals*, **2019**, 9, 364.
[101] J. J. Gao, P. M. Guo, Y. H. Qi, D. L. Yan, *J. Iron Steel Res.* **2011**, 23, 14.
[102] W. Zhang, Z. L. Xue, J. H. Zhang, W. Wang, C. G. Cheng, Z. S. Zou, *J. Iron Steel Res. Int.* **2017**, 24, 778.
[103] W. Zhang, *Doctoral Thesis*, Northeastern University, **2015**.
[104] I. Muchi, J. Yagi, K. Tamura, *J. Japan Inst. Metals* **1966**, 30, 826.
[105] P. B. Abhale, N. N. Viswanathan, H. Saxén, *Min. Proc. Extr. Metall.* **2020**, 129, 166.
[106] J. W. Yin, F. Q. Wang, T. H. Dang, J. L. Zhang, Z. K. Gao, *J. Iron Steel Res.* **2002**, 14, 1.
[107] X. J. Zuo, J. S. Wang, X. W. An, X. F. She, Q. G. Xue, *J. Iron Steel Res. Int.* **2013**, 20, 12.
[108] R. Z. Lan, J. S. Wang, Y. H. Han X. F. She, L .T. Wang, Q. G. Xue, *J. Iron Steel Res. Int.* **2012**, 19, 13.
[109] Z. Qiao, H. J. Zhang, J. S. Wang, *J. Taiyuan Univ. Technol.* **2014**, 45, 25.
[110] J. Li, P. Wang, L. Zhou, M. Cheng, *ISIJ Int.* **2007**, 47, 1097.
[111] L. Chen, Q. G. Xue, W. T. Guo, X. F. She, J. S. Wang, *Ironmak. & Steelmak.* **2016**, 43, 458.
[112] G. Wang, Y. L. Liu, Z. F. Zhou, J. S. Wang, Q. G. Xue, *JOM* **2018**, 70, 29.
[113] P. Wang, J. Li, L. Zhou, H. Long, *Ironmak. & Steelmak.* **2013**, 40, 312.
[114] P. Wang, Y. Wu, Q. M. Meng, Z. X. Di, *Ironmak. & Steelmak.* **2019**, 47, 290.
[115] Y. F. Chai, J. L. Zhang, Q. J. Shao, *High Temp. Mater. Proc.* **2019**, 38, 42.
[116] D. Senk, H. W. Gudenau, S. Geimer, E. Gorbunova, *ISIJ Int*. **2006**, 46, 1745.
[117] I. G. Tovarovskii, A. P. Pukhov, Y. S. Yusfin, *Steel in the USSR* **1989**, 19, 328.
[118] B. Wright, P. Zulli, Z. Y. Zhou, A. B. Yu, *Powder Technol.* **2011**, 208, 86.
[119] Z. Y. Zhou, H. P. Zhu, B. Wright, A. B. Yu, P. Zulli, *Powder Technol.* **2011**, 208, 72.
[120] G. Danloy, A. Berthelemot, M. Grant, *Rev. Met.* **2009**, 106, 1.
[121] Qi, Y.H.; Yan, D.L.; Gao, J.J.; Zhang, J.C.; Li, M.K. Study on industrial test of the oxygen blast furnace. *Iron & Steel* **2011**, 46(3), 6-8.
[122] Y. H. Qi, J. I. Gao, Y. S. Zhou, presented at *the 7th Metallurgical energy conservation and low carbon technology seminar*, Tangshan, September **2011**.
[123] T. Matsumiya, *CALPHAD* **2011**, 35, 627.
[124] S. Watakabe, K. Miyagawa, S. Matsuzaki, T. Inada, Y. Tomita, K. Saito, M. Osame, P. Sikström, L. S Ökvist, J. O. Wikstrom, *ISIJ Int*. **2013**, 53, 2065.

[125] China metallurgical News, **2020**-07-17. https://wemp.app/posts/7b1b8d27-71bf-481e-b213-f111ca690e3b.

[126] W. H. Li, T. Li, *Xinjiang Iron & Steel*, **2020**, 153, 1.

[127] E. Nduagu, I. Romão, J. Fagerlund, R. Zevenhoven, *Appl. Energ.* **2013**, 106, 116.

[128] R. Zevenhoven, M. Slotte, J. Åbacka, J. A. Highfield, *Energy*, **2016**, 117, 604.

[129] R. Zevenhoven, M. Virtanen, *Energy*, **2017**, 141, 2484.

[130] G. Léonard, *Doctoral Thesis*, University of Liège, **2013**.

[131] G. Mondino, *Master's Thesis*, Politecnico di Torino, **2013**.